AFRL-OSR-VA-TR-2015-0028

Development of Detailed and Reduced Kinetic Mechanisms

Fokion Egolfopoulos
UNIVERSITY OF SOUTHERN CALIFORNIA LOS ANGELES

12/04/2014
Final Report

Air Force Research Laboratory
AF Office Of Scientific Research (AFOSR)/ RTE
Arlington, Virginia 22203
Air Force Materiel Command

REPORT DOCUMENTATION PAGE

Form Approved
OMB No. 0704-0188

1. REPORT DATE *(DD-MM-YYYY)*	**2. REPORT TYPE**	**3. DATES COVERED** *(From - To)*
30-11-2014	Final Technical	1-9-2011 - 31-8-2014

4. TITLE AND SUBTITLE

(U) Development of Detailed and Reduced Kinetics Mechanisms for Surrogates of Petroleum-Derived and Synthetic Jet Fuels

5a. CONTRACT NUMBER

5b. GRANT NUMBER
FA9550-11-1-0217

5c. PROGRAM ELEMENT NUMBER
61102F

6. AUTHOR(S)
Fokion N. Egolfopoulos

5d. PROJECT NUMBER
2308

5e. TASK NUMBER
BX

5f. WORK UNIT NUMBER

7. PERFORMING ORGANIZATION NAME(S) AND ADDRESS(ES)
University of Southern
California
Los Angeles, CA 90089

8. PERFORMING ORGANIZATION REPORT NUMBER

9. SPONSORING / MONITORING AGENCY NAME(S) AND ADDRESS(ES)

875 Randolph Street
Suite 325, Room 3112
Arlington, VA 22203-1768

10. SPONSOR/MONITOR'S ACRONYM(S)

11. SPONSOR/MONITOR'S REPORT NUMBER(S)

12. DISTRIBUTION / AVAILABILITY STATEMENT

Approved for public release; distribution is unlimited

13. SUPPLEMENTARY NOTES

14. ABSTRACT

The oxidation and pyrolysis of a variety of fuels of relevance to air breathing propulsion were studied experimentally behind reflected shock waves, in flow reactors, as well as in laminar and turbulent flames. The measurements included ignition delays and species time evolutions in shock tubes, species profiles in flow reactors, and propagation speeds and ignition/extinction limits of laminar flames. Additionally, a facility was constructed that allows for the study of turbulent flames at very high Re numbers and fuels as heavy as n-dodecane. The main goal of the completed program was to identify the important kinetic pathways of jet fuel pyrolysis and oxidation under conditions that mimic those encountered in jet engines, and to develop appropriate models for real fuels based on the experimental data. This was a collaborative three-year research effort between the following universities and investigators: University of Southern California: F.N. Egolfopoulos (PI), H. Wang (co-PI); Drexel University: N.P. Cernansky (co-PI), D.L. Miller (co-PI); Princeton University: C.K. Law (co-PI); Stanford University: C.T. Bowman (co-PI), R.K. Hanson (co-PI), H. Wang (co-PI).

15. SUBJECT TERMS

Ignition, Fuel Oxidation, Flame Propagation, Flame Extinction, Flame Kinetics, Transport Theories, Surrogate Jet Fuels

16. SECURITY CLASSIFICATION OF:			**17. LIMITATION OF ABSTRACT**	**18. NUMBER OF PAGES**	**19a. NAME OF RESPONSIBLE PERSON**
a. REPORT	**b. ABSTRACT**	**c. THIS PAGE**			Chiping Li
Unclassified	Unclassified	Unclassified	UL	55	**19b. TELEPHONE NUMBER** *(include area code)* (703) 696-8574

Final Technical Report

DEVELOPMENT OF DETAILED AND REDUCED KINETICS MECHANISMS FOR SURROGATES OF PETROLEUM-DERIVED AND SYNTHETIC JET FUELS

(AFOSR Grant FA9550-11-1-0217)

(Period: September 1, 2011 – August 31, 2014)

FOKION N. EGOLFOPOULOS

Department of Aerospace & Mechanical Engineering

University of Southern California

Los Angeles, California 90089-1453

Summary/Overview

The oxidation and pyrolysis of a variety of fuels of relevance to air breathing propulsion were studied experimentally behind reflected shock waves, in flow reactors, as well as in laminar and turbulent flames. The measurements included ignition delays and species time evolutions in shock tubes, species profiles in flow reactors, and propagation speeds and ignition/extinction limits of laminar flames. Additionally, a facility was constructed that allows for the study of turbulent flames at very high Re numbers and fuels as heavy as *n*-dodecane. The main goal of the completed program was to identify the important kinetic pathways of jet fuel pyrolysis and oxidation under conditions that mimic those encountered in jet engines, and to develop appropriate models for real fuels based on the experimental data.

This was a collaborative three-year research effort between the following universities and investigators:

1. University of Southern California: F.N. Egolfopoulos (PI), H. Wang (co-PI);
2. Drexel University: N.P. Cernansky (co-PI), D.L. Miller (co-PI);
3. Princeton University: C.K. Law (co-PI);
4. Stanford University: C.T. Bowman (co-PI), R.K. Hanson (co-PI), H. Wang (co-PI).

Technical Discussion

1.0 Background

As described in the research proposal, the problems being tackled can be grouped into two categories: (1) understanding and quantifying the combustion properties of practical fuels used in air-breathing propulsion systems and selection of appropriate surrogate fuels; and (2) developing reliable detailed reaction models and strategies for model reduction for use in large-scale simulations. The research is a natural extension of the numerous experimental, theoretical, and modeling contributions that have been made in the past by the PIs. The proposed research concerns two types of jet fuels. The first is conventional petroleum-derived "reference" JP-8 fuels. The second is non-petroleum-derived or synthetic jet fuels. By considering these two types of fuels, both short-term (current fuels and systems) and potential long-term (fuel-flexible energy conversion and design) needs of air-breathing propulsion are addressed.

The research efforts of the completed program are directly relevant to the research focus on key combustion phenomena and characteristics, including flame propagation, flammability limits, and combustion instabilities in turbulent flames, and relevant also to at least three objectives stated in Section 11 objectives that are highlighted in Section 11 (Energy Conversion and Combustion Sciences) of AFOSR BAA-AFOSR-2012-0001:

- In the area of turbulent combustion: "validating as directly as possible and further developing basic model assumptions used in the numerical simulation for turbulence combustion."

- In the area of combustion modeling and theory: "using numerical simulations as an experimental tool (numerical experiments), with help of theoretical combustion research, to qualitatively explore key combustion phenomena to obtain fundamental understanding and to identify rate-controlling processes and scales in different ranges of flow (including turbulence) and fueling conditions."

- In the area of combustion modeling and theory: “analytical and numerical approaches to simplify and reduce complex mathematical systems applicable to combustion modeling.”

Combustion reaction kinetics is an integral part of any effort towards achieving basic understanding of turbulent flame phenomena. Specifically, reaction kinetics plays a critical role in flame propagation, extinction, and re-ignition. These phenomena are related directly to turbulent flame propagation, flammability limits, and instabilities. Hence, the long-term impact of the completed program becomes clearer as the kinetic models that are developed will be of relevance to the reacting conditions encountered in high-speed aero-propulsion.

For example, the results are useful in examining the assumptions adopted in constructing turbulent flame regime diagrams. A prevailing paradigm of turbulent combustion research is the classification of the combustion regimes in terms of turbulent time scales. A key assumption is that such a classification can be made with a limited number of parameters characterizing the large-scale turbulent velocity and spatial scales. The basis of this approach is the work of Damköhler (1940), who postulated that turbulence simply wrinkles the thin reaction layer that exhibits a laminar flame-like structure. This description led to the concept of flamelets, which appear to exist in all cases accessible by available imaging techniques even at high turbulence intensities. Within the realm of this description, a property critical to characterizing the behaviors of turbulent flames is the turbulent flame speed. As discussed by Bray and Cant (1991), this property appears to scale with the laminar flame speed through the flamelet surface area density, flame brush thickness, and flame stretch. Yet this concept was derived largely based on experimentation on turbulent flames burning hydrogen and small hydrocarbons, i.e. methane. The aforementioned underlying assumption has yet to be examined in the context of large, complex hydrocarbon fuels.

It is known that turbulence broadens the preheat zone of a flamelet in such a way that the reaction kinetics of fuel cracking may be impacted severely just ahead of the flame sheet. Fuel cracking alters the unburned gas composition. It is also expected that turbulence will promote mixing of burned gases and unburned reactants to various extents depending on the turbulent intensity thus modifying the reactant composition even before entering the preheat zone. Both

phenomena could cause the flame sheet to assume a local flame speed that cannot be predicted easily at present. Also, it remains unclear as to what extent changes in the local flame speed impact the global turbulent flame speed.

The results of the completed program will have long-term impact on air-breathing propulsion, and it is relevant to the current AFOSR research focus by introducing new directions and as a result new additional experiments that aim to provide insight into the effects of fuel type and its heating time history. Thus, the deliverables provide a roadmap towards the development of kinetic models that will be relevant to conditions encountered in high-speed applications.

2.0 Objectives

The main objectives of the proposed work are shown below. The fuels that were considered included petroleum-derived or synthetic jet fuels, as well as selected *n*-alkanes, *iso*-alkanes, *cyclo*-alkanes, and aromatics that are of relevance either to the traditional formulation of surrogates or to the products of fuel decomposition due to turbulence as outlined below.

1. High Re number, turbulent premixed jet flame experiments. A piloted premixed jet burner (PPJB) was used to achieve Re numbers as high as 100,000 for gaseous and heavy liquid fuels. These experiments aimed to provide evidence of the effect of fuel chemistry on turbulent combustion by implementing various diagnostics such as:

    - Direct flame luminosity visualization for determining the average topology of the (luminous) reaction zone;

    - Shadowgraph for determining the average and instantaneous topology of regions of density gradients that, in combination with velocity field data, could be used to extract information about the preheat zone;

    - Particle image velocimetry (PIV) for velocity measurements that will provide information regarding the mean and rms flow velocities, energy and dissipation spectra, as well as the predominant components of the strain rate tensor and their higher moments;

2. Quantification of effects of preheat-zone fuel cracking on local flame properties. The approach included detailed numerical simulations and search of a low dimensional space that could be used to describe the controlling chemical processes under a wide range of conditions as encountered in a highly turbulent flow field.

3. Studies of fundamental flame properties of products of fuel decomposition. The preheat zone fuel cracking studies provided information regarding the smaller hydrocarbons that result from the fuel decomposition and which are fed into the flame.

4. Shock tube studies of fuel pyrolysis and oxidation. Existing and new shock tube and laser absorption techniques were applied to investigate the pathways and rates for pyrolysis and oxidation of jet fuel surrogates, in collaboration with flow reactors studies. Of particular interest and novelty was the development of new experimental strategies that provide insight and high-quality data in several possible areas: the formation and reaction of radical species; the rate of change of chemical energy during reaction; and the behavior of fuels under variable heating profiles.

5. Low- and high-temperature flow reactor tube studies of fuel pyrolysis mimicking the conditions of the preheat zone. Fuel pyrolysis (and oxidation) pathways were studied in flow reactors at different temperatures. While high temperatures are expected to dominate the fuel initial decomposition, lower temperature regimes are expected also to be important in locations close to the fuel injection region. The time scales in the high-temperature flow reactor can be small and of relevance to those encountered in high Re flows. On the other hand the time scales in the low temperature flow reactor can be large and not relevant to the problem at hand, and thus additives could be used to accelerate the pertinent time scales.

3.0 Summary of Completed Tasks

3.1 Flow Reactor Studies, Drexel University

- Oxidation at 550-850 K and pressure of 8 atm.
    - *n*-PCH: Equivalence Ratio of 0.27±0.05;
        - Relatively low contribution of cyclic species to carbon balance: suggests backbone ring opening is the preferred path.
    - 2,7-DMO: Equivalence Ratio of 0.31±0.05.
        - Two tertiary C-H sites: pathways significant production of iso-butene.
- Pyrolysis at 850-1000 K and pressure of 8.0 atm.
    - *n*-Decane: 900±50 ppm *n*-Decane with Balance N_2;
        - C_2-C_{10} alkenes measured with lighter species existing at higher levels.
    - *n*-Dodecane: 781±9 ppm *n*-Decane with Balance N_2.
        - C_2-C_{12} alkenes measured with lighter species existing at higher levels.

3.1.1 Experimental Approach

The Pressurized Flow Reactor (PFR) at Drexel University is a turbulent flow reactor designed to study the low (< 650 K) to intermediate temperature (650-1000 K) oxidation of hydrocarbon fuels with relative isolation from physical phenomena such as gradients in temperature and the flow field (Koert and Cernansky, 1992). The PFR contains a 22.5 mm ID, 40 cm long quartz reactor tube to provide a reaction environment with minimal surface effects. The quartz reactor tube is contained within a stainless steel pressure vessel for pressure elevation up to a maximum of 9.5 atm. The volume between the quartz reactor tube and pressure vessel forms an annulus that is at the same pressure as the reaction chamber. Synthetic air and high-

pressure pre-vaporized fuel/nitrogen are introduced into an opposed jet annular mixing nozzle at the inlet to the quartz reactor tube. A water-cooled, borosilicate glass-lined stainless steel sample probe extracts and quenches samples from the centerline of the quartz reactor tube and it contains an integrated type-K thermocouple. Figure 1 depicts the schematic of the PFR equipment and setup.

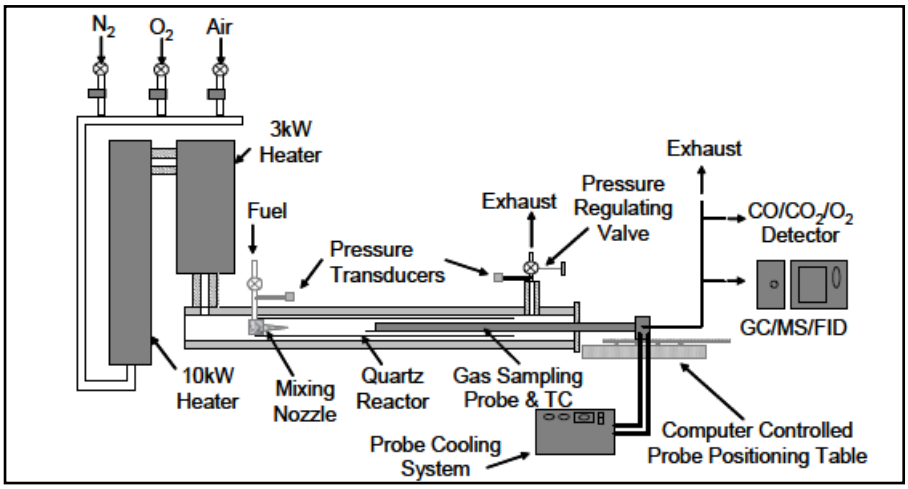

Figure 1. Pressurized Flow Reactor (PFR) schematic.

A Direct Transfer Controlled Cool Down (DT-CCD) methodology is used to minimize the time duration between sample collection and analysis in the GC/MS/FID (Kurman, 2010). The PFR is heated to the maximum desired reaction temperature of approximately 850 K using pre-heated air from the circulation heaters. Upon reaching the maximum reaction temperature, fuel is injected into a heated nitrogen stream to ensure vaporization prior to entering the mixing nozzle where it is rapidly mixed with synthetic air in the opposed jet annular mixing nozzle. Further dilution with nitrogen is used to limit temperature rise from heat release. To maintain a constant residence time during the controlled cool down, the sample probe is repositioned for each sample. While the GC/MS/FID analysis is performed on the first sample, the PFR temperature is decreased to the next sample temperature. CO and CO_2 concentration is determined with an on-line, continuous NDIR analyzer and O_2 is measured using an electrochemical oxygen sensor.

3.1.2 Modelling Approach

Note: The Phase I Final Report only had a generic explanation of Jetsurf and other modeling details in this section and there were not separate sub-sections for each university. We assume that the same approach will be followed for the Phase II final report as well.

3.1.3 Results and Discussion

3.1.3.1 Low Temperature Oxidation of *n*-Propylcyclohexane and 2,7-Dimethyloctane

The pressurized flow reactor (PFR) at Drexel University was used to study the low temperature oxidation of *n*-Propylcyclohexane (*n*-PCH) / air and *2,7*-Dimethyloctane (*2,7*-DMO) / air (Corrubia et al., 2011; Farid et al., 2013). *n*-PCH was studied to complement the previous *n*-BCH studies to investigate the effect of alkyl side chain length. The following results for *n*-PCH oxidation were obtained by performing two PFR experiments at nearly identical conditions, as shown in Table 1.

Table 1. Test conditions for *n*-PCH oxidation, residence time 120±10 ms.

Parameter	Exp 1	Exp 2	Avg	Uncertainty
***n*-PCH, ppm**	830	821	826	±20
O_2 , ppm	42,100	42,100	42,100	±1250
N_2	Balance	Balance	Balance	-
Equivalence Ratio (ϕ)	0.27	0.27	0.27	±0.05
Temperature, K	550-850	550-850	550-850	-
Pressure, atm	8.000	8.000	8.000	±0.025

Figure 2 shows the reactivity map for *n*-PCH oxidation, manifested by carbon dioxide production, along with the molar fractions of carbon dioxide, molecular oxygen, and *n*-PCH plotted with respect to temperature.

Seventy intermediate species were identified and quantified with the GC/MS/FID system during both experiments. The carbon balances for all sample temperatures were greater than 90%, with the minimum occurring at the 700 K temperature sample point. Figure 3 presents the key linear alkenes measured during *n*-PCH oxidation. In addition to ethene, propene, and butene, pentene, hexene and alkynes (i.e. 2-butyne) were also measured at much smaller molar fractions of less than approximately 1 ppm.

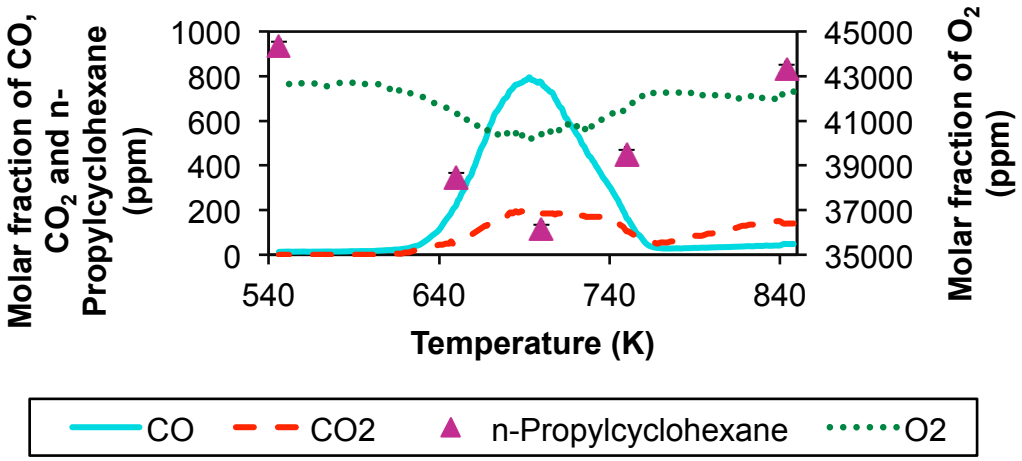

Figure 2. Reactivity map for *n*-PCH oxidation.

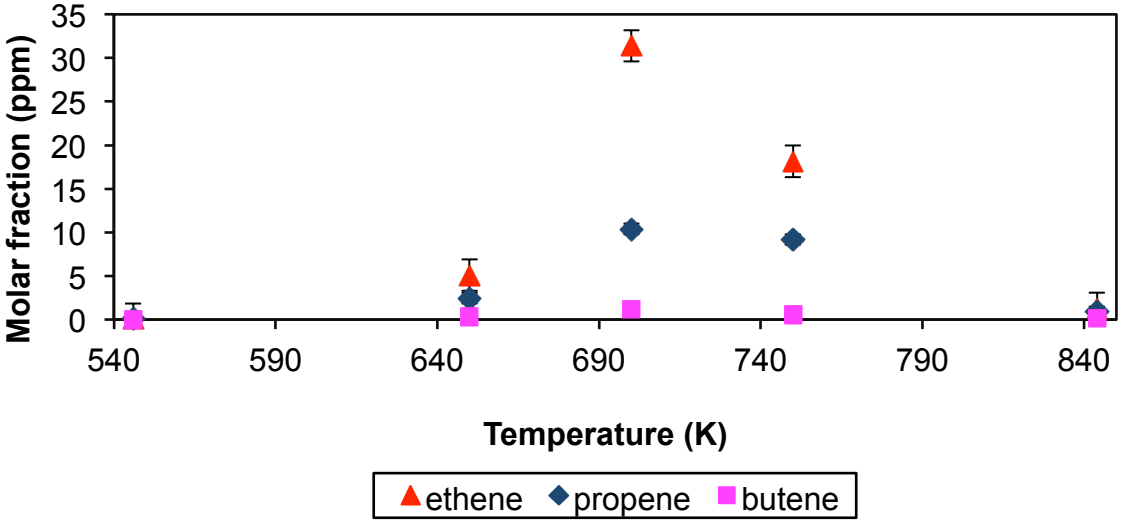

Figure 3. Key alkenes for *n*-PCH oxidation.

Three replicate experiments for *2,7*-dimethyloctane were conducted. The experimental conditions and the uncertainties are shown in Table 2.

Table 2. Test conditions for 2,7-DMO oxidation, residence time 120±10 ms.

Parameter	Exp 1	Exp 2	Exp 3	Avg	Uncertainty
2,7-DMO, ppm	843	856	830	843	±13
O_2 , ppm	42,100	42,100	42,100	42,100	±1250
N_2	Balance	Balance	Balance	Balance	-
Equivalence Ratio (ϕ)	0.30	0.32	0.31	0.31	±0.05
Temperature, K	550-850	550-850	550-850	550-850	-
Pressure, atm	8.000	8.000	8.000	8.000	±0.025

2,7-DMO exhibited classical NTC behavior as indicated by the reactivity map, shown in Fig. 4. Figure 5 shows the major alkenes identified and quantified, listed in order of decreasing molar fraction at 750 K were as follows: iso-butene, propene, 2-methyl-1-pentene and ethene. iso-Butene is a major intermediate species produced during the oxidation of *2,7*-DMO. The stability of butene is possibly a reason for the lower overall reactivity of *2,7*-DMO compared with the straight chain alkane of same carbon number (i.e., *n*-Decane) when comparing CO molar fraction for both fuels at similar experimental conditions in the PFR. The 2-methyl-1-pentene intermediate was possibly produced via C-C bond scission of *2,7*-DMO due to the similar chemical structure and methyl group being present in both species. In addition, it was observed that chain branching affects the level distribution of C_2-C_4 alkene intermediates. While the oxidation of *n*-decane resulted primarily in the formation of ethylene near the NTC start, propene and iso-butene were the major olefins produced from *2,7*-DMO.

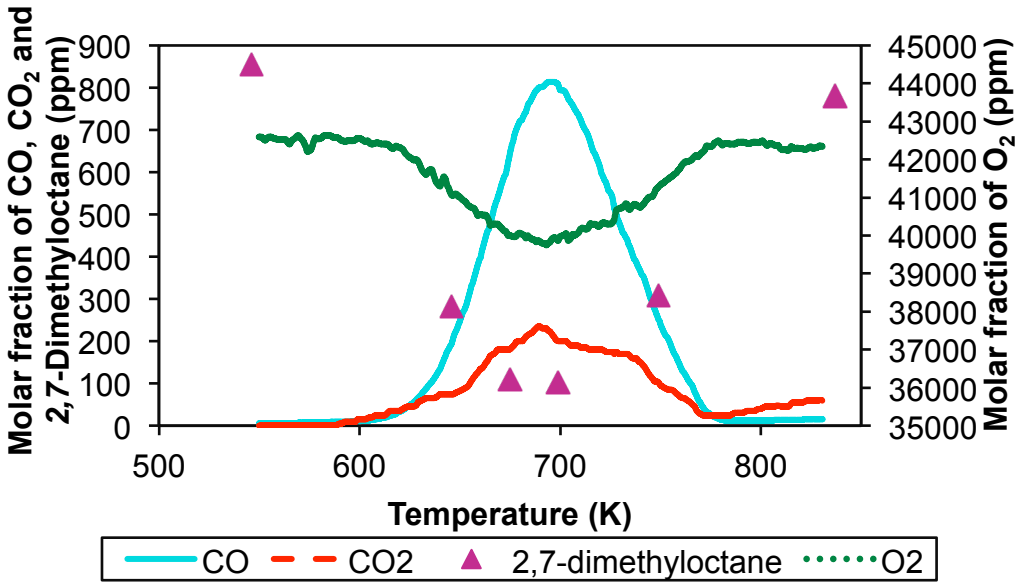

Figure 4. Reactivity map for *2,7*-DMO oxidation.

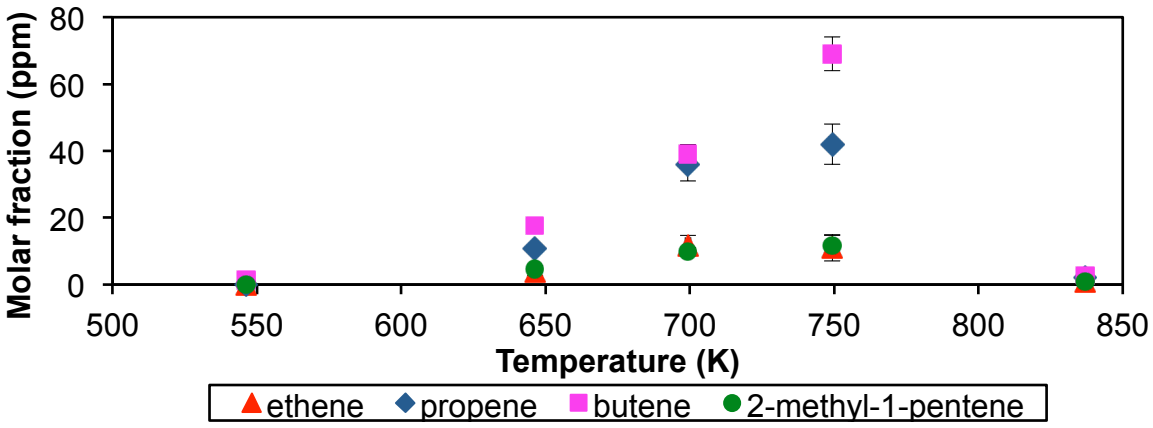

Figure 5. Key alkenes for *2,7*-DMO oxidation.

3.1.3.2 Intermediate Temperature Pyrolysis of *n*-Decane and *n*-Dodecane

During the modified scope of phase II efforts, the PFR was used to measure the stable intermediates produced from decomposition of select jet fuel surrogate components. Two pyrolysis experiments with *n*-decane and two pyrolysis experiments with *n*-dodecane were performed. In these tests, decomposition of both fuels was examined at a pressure of 8 atm, temperature range of 850 - 1000 K and a residence time of 168 ms. The main goal of these experiments was to examine the extent to which these fuel components break into smaller species at the studied conditions. Table 3 and Table 4 depict the test conditions for each fuel.

Table 3. Test conditions for *n*-decane pyrolysis, residence time 168±10 ms.

Parameter	$C_{10}P1$	Uncertainty	$C_{10}P2$	Uncertainty
n-decane, ppm	856	±39	990	±46
N_2	Balance	-	Balance	-
Temperature, K	850, 1000	-	850, 1000	-
Pressure, atm	8.000		8.000	±0.025
Residence time, ms	168	±10	168	±10

Table 4. Test conditions for *n*-dodecane pyrolysis, residence time 168±10 ms.

Parameter	$C_{12}P1$	Uncertainty	$C_{120}P2$	Uncertainty
n-dodecane, ppm	781	±9	749	±51
N_2	Balance	-	Balance	-
Temperature, K	850 – 1000*	-	850 – 1000	-
Pressure, atm	8.000		8.000	±0.025
Residence time, ms	168	±10	168	±10

* Samples extracted at 50 K intervals (850 K, 900 K, 950 K and 1000 K)

Figure 6 compares the predictions of two chemical kinetic mechanisms, LLNL 2011 and optimized JetSurf, with those measured during the second experiment with *n*-decane ($C_{10}P2$). As seen, the models considerably overestimate *n*-decane consumption. While only about 15% of *n*-decane was consumed at 1000 K sample point, the model predicts that about 50% of *n*-decane would be consumed at a sample temperature of 1000 K. The models also overestimate the production of ethylene at 1000 K sample temperature.

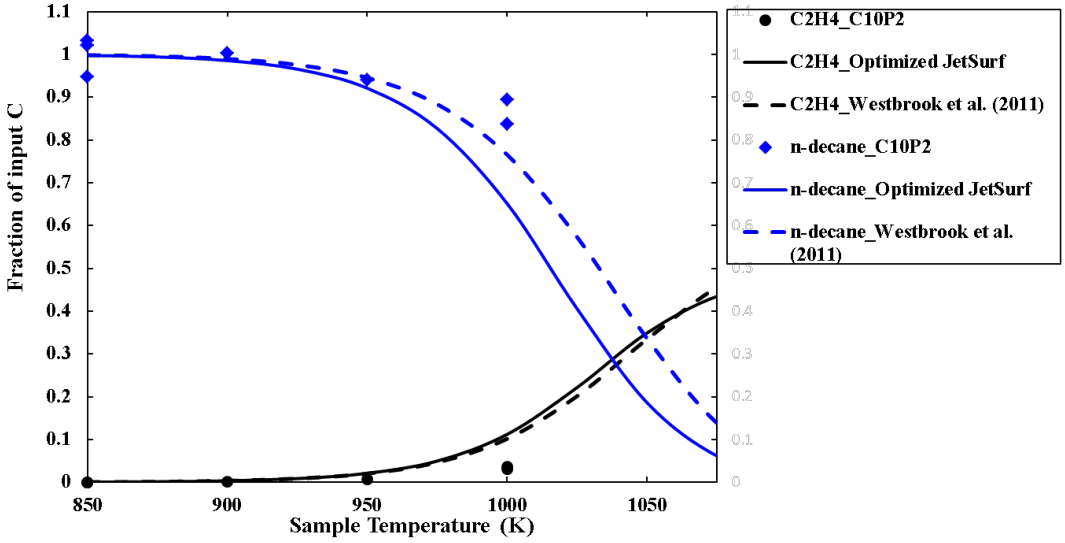

Figure 6. Intermediate-T pyrolysis of *n*-decane – $C_{10}P2$ vs. simulations.

Figure 7 illustrates a comparison between the first experimental study of *n*-dodecane ($C_{12}P1$) with two chemical kinetic models, LLNL 2011 and optimized JetSurf. As seen, both models overestimate fuel consumption. While less than 15% of *n*-dodecane was consumed at 1000 K sample point, the optimized JetSurf predicts that more than 60% of *n*-dodecane would be consumed at 1000 K. Both models and the experiment agreed on production of ethene from *n*-dodecane pyrolysis. The models also agreed with the experiment in predicting a decrease in concentration of alkenes with an increase in their molecular size. Both models however, largely overestimated the concentration of alkenes produced at 1000 K sample point (only ethene shown in Fig. 7.).

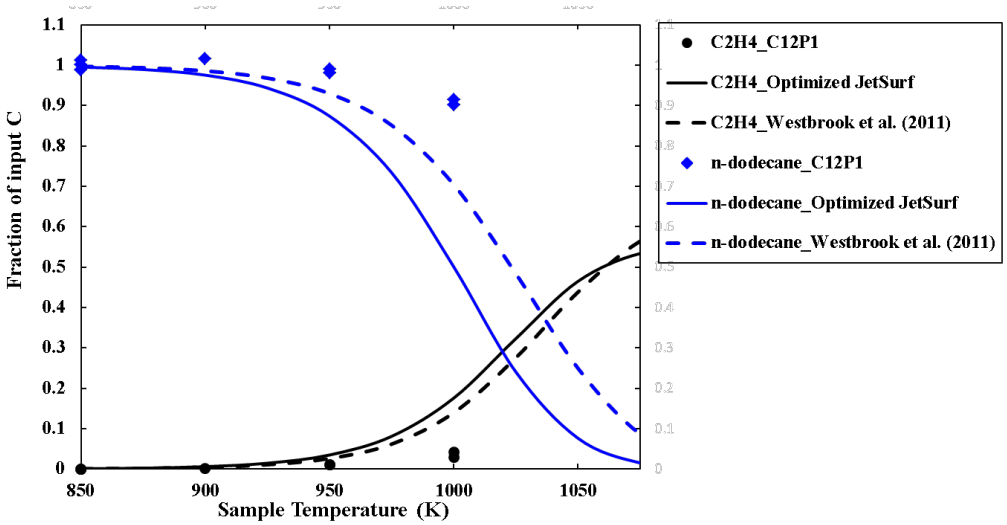

Figure 7. Intermediate-T pyrolysis of *n*-dodecane – $C_{12}P2$ vs. simulations.

3.2 Flow Reactor Studies, Stanford University

- Modified an existing variable-pressure flow reactor for operation using liquid fuels.
- Conducted experiments on the pyrolysis and oxidation of *n*-dodecane over a range of temperatures, stoichiometries and pressures.
- Compared experimental data with model predictions using the JetSurf reaction mechanism (Banerjee et al, 2014a, 2014b).

3.2.1 Pressurized Flow Reactor, Stanford University

The experiments were conducted in a variable pressure flow reactor, shown in Fig. 8.

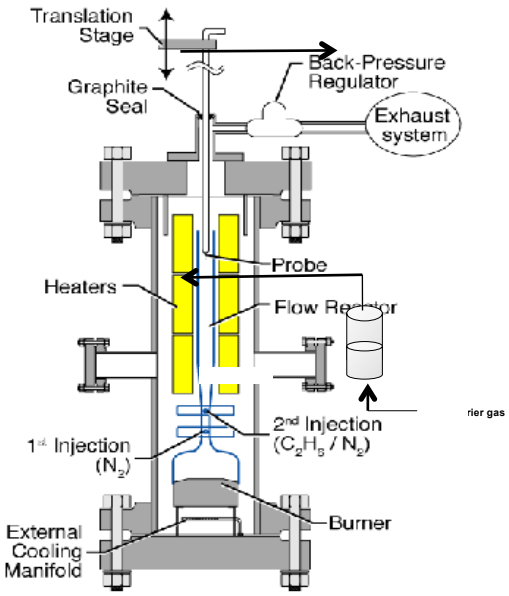

Figure 8. Variable pressure flow reactor.

Liquid *n*-dodecane, vaporized in an evaporator in a thermostated bath, is carried to the flow reactor by a N_2 carrier gas and injected through a series of radial injectors into flowing combustion products from a premixed flame burner operating on $H_2/O_2/N_2$. Upstream of the fuel injectors is another set of radial injectors in which N_2 is injected into the combustion products.

Controlling the flow rates of H_2, O_2, N_2 and the fuel/N_2 mixture fixes the temperature and stoichiometry of the reactant mixture at the entrance to the constant-area flow reactor. Three electrical heating elements located along the length of the reactor maintain the reactor at nearly adiabatic conditions. The concentrations of stable product species and temperature are measured on the centerline along the length of the reactor using traversing an extractive sampling probe and a thermocouple probe, respectively. The extracted gas sample is transferred through a heated sample line to online analyzers for analysis. Oxygen in the sample is measured using a paramagnetic analyzer; stable carbon-containing species are measured using either NDIR analyzers or by gas chromatography. All flow rates and data acquisition are computer controlled via a PC with LabVIEW software. The temperature range of the present experiments ranges between 1000 - 1250K; pressure of 1 atm; stoichiometries range from 0.5 (lean) - 1.5 (rich) in the oxidation experiments.

3.2.2 Results and Discussion

Representative experimental results for *n*-dodecane oxidation and comparisons with simulated profiles using the JetSurf 1.0 reaction mechanism are shown in Figs. 9, 10, and 11.

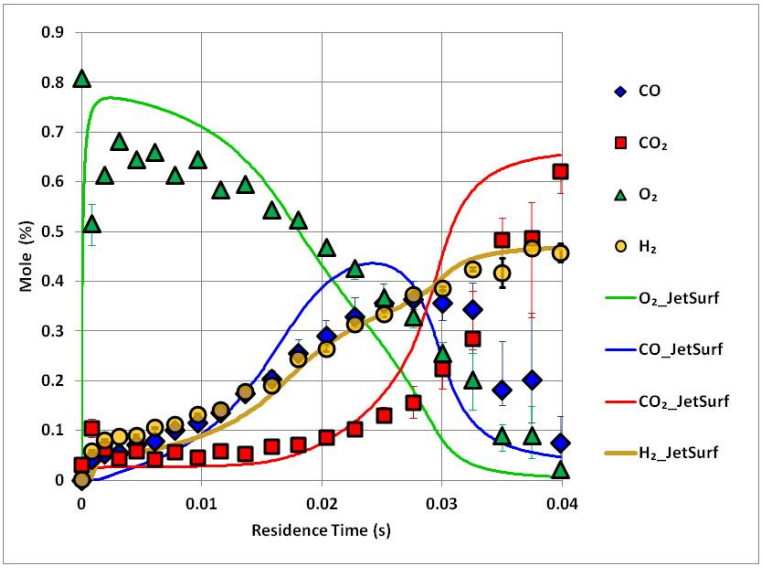

Figure 9. Comparison of measured and calculated profiles of CO, CO_2 and O_2 for T = 1220K, p = 1 atm, and 290 ppm *n*-$C_{12}H_{26}$/8600 ppm O_2.

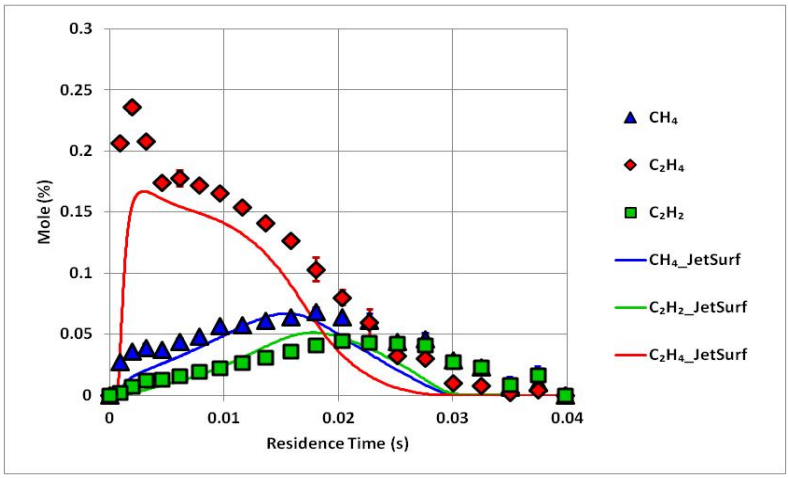

Figure 10. Comparison of measured and calculated profiles of CH_4, C_2H_2, and C_2H_4 for the conditions of Fig. 11.

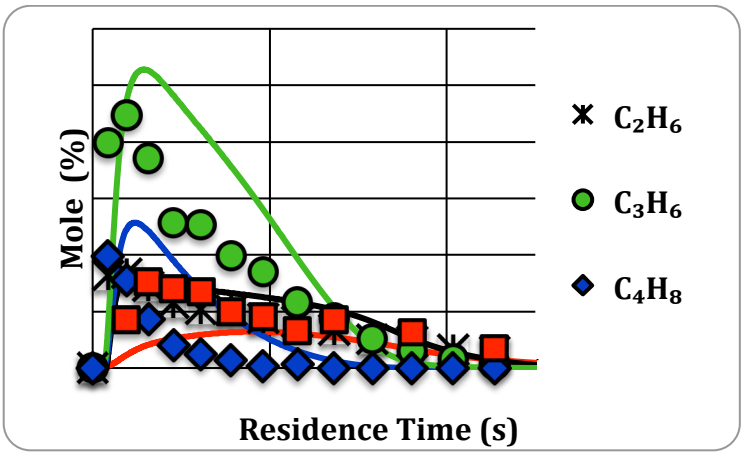

Figure 11. Comparison of measured and calculated profiles of C_2H_6, C_3H_6, and C_4H_8 and CH_2O for the conditions of Fig. 11.

The comparisons of measured species profiles with profiles calculated using Jet Surf 1.0 indicate that the calculated reaction time scales are somewhat smaller than the measured ones. In addition, the removal of the *n*-dodecane is so rapid that is below measurable quantities at the first measurement station and prior to any change in the O_2 mole fraction. The principal products of the *n*-dodecane decomposition are C_2H_4, CH_4, C_3H_6 and H_2. Subsequent oxidation of these species leads to formation of CO and CO_2 on a much slower time scale. The observation of the

rapid removal of the *n*-dodecane prior to any removal of O_2 motivated a study of the pyrolysis of *n*-dodecane. Representative results from these experiments are shown in Fig. 12.

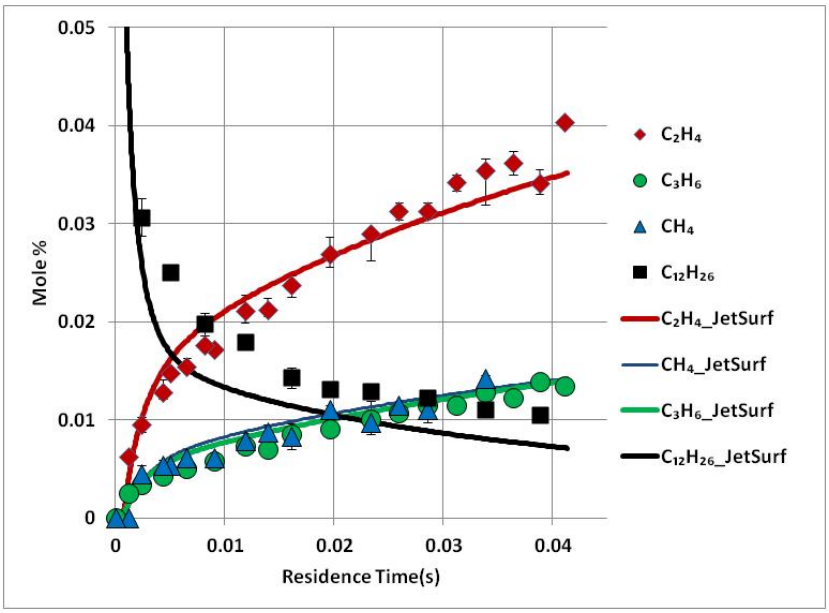

Figure 12. Comparison of measured and calculated profiles of $C_{12}H_{26}$, C_2H_4, C_3H_6 and CH_4 for pyrolysis of *n*-dodecane at 1000 K and 1 atm.

The JetSurf model reproduces the experimental results. The primary decomposition products are the same as are observed in the oxidation experiments, viz. C_2H_4, CH_4 and C_3H_6. Further details on this study may be found in Banerjee et al. (2014a, 2014b).

3.3 Shock Tube Studies, Stanford University

- Ignition Delay Times for a Series of Branched Alkanes (Li et al. 2014).
- Ignition Delay Times and Pyrolysis Species Time Histories for Decalin (Zhu et al. 2014).
- Ignition Delay Times for Propene (Burke et al. 2014)
- Ignition Delay Times and Pyrolysis Species Time Histories for 2,7-Dimethyloctane (Li et al. in press).

3.3.1 Shock Tube Facility

Experiments were performed in either the 14 cm I.D. Kinetics Shock Tube or the 5 cm I.D. High Pressure Shock Tube (HPST) at Stanford. The Kinetics Shock Tube has an electro-polished stainless steel driven section with length/diameter (L/D) ratio of 70 and used a helium-filled driver section with an L/D of 30 to burst 0.25 mm thick polycarbonate diaphragms (against a crossed-knife arrangement in a short square section of the shock tube). The shock tube is sealed with Viton O-rings, is operated at room temperature (i.e. without heating) and can be turbo-pumped overnight to an ultimate pressure ~ 10^{-6} torr and to a leak and outgassing rate of ~ $3x10^{-6}$ torr/min. Typically reflected shock wave experiments were performed hourly and over this time frame the ultimate shock tube pressure before filling was ~ $5x10^{-6}$ torr and the leak and outgassing rate was ~10^{-5} torr/min.

Test gas mixtures were stored in a 40 liter stainless steel tank heated uniformly to 60 ^{o}C, and mixed with a magnetically-driven stirring vane. Mixtures were made using partial pressures and pre-shock filling concentrations in the shock tube were confirmed using *in situ* 3.39 micron laser absorption. 99.999% Argon and 99.99% oxygen (Praxair) were used with spectroscopic grade hydrocarbon fuel samples (99.5+%) (Sigma-Aldrich) with no further preparation except for vacuum pumping to removed dissolved volatiles and oxygen.

Incident shock speeds were determined by extrapolating, to the end wall position, shock velocities measured over the last 2 meters of the driven section. Reflected shock conditions were calculated using a standard chemically frozen shock code and standard thermo-chemical data. Resulting uncertainties in reflected shock temperatures over test times of 1 ms were <±1%.

High pressure experiments are performed in the HPST. This shock tube is designed to allow experiments up to and above 500 atm. It is heated (up to 150^{o}C) and is it mixing assembly.

Laser Absorption Measurements

IR He-Ne laser absorption of fuel: Fuel mole fraction was monitored with IR He-Ne laser absorption at 3.39 μm. A C-H stretch vibrational absorption feature for many hydrocarbons extends across this wavelength. For certain species, large alkanes in particular, absorption at this wavelength is relatively strong; and absorption by smaller hydrocarbon species, and in particular, alkenes, is weaker. Thus, at early times the absorption at 3.39 μm is dominated by the absorption by *n*-dodecane and this measurement can be used to monitor the fuel time-history. At later times, after the majority of the fuel has decomposed, the residual absorption signal is dominated by the decomposition products with the highest absorption cross-section – mole fraction product. Relatively accurate fuel profiles over the entire experimental timeframe are possible, if corrections to the 3.39 μm absorption profiles based on subtraction of ethylene (and higher alkene interfering species) are included. High-temperature absorption cross-sections of selected fuels and their decomposition products, and experimental details of this method, are discussed in Klingbeil et al. (2006).

CO_2 laser absorption of C_2H_4: Ethylene mole fraction was monitored by taking advantage of the fortuitous overlap of the P(14) line of the CO_2 gas laser at 10.532 microns with the strong ethylene absorption band near 10.6 microns. Similar to the situation with the C-H stretch absorption band near 3.39 microns, there is a wide CH_2 wag absorption feature near 10.6 microns that is shared in varying (but weaker) strengths (at the P(14) line in particular) by other alkenes (e.g. ethylene, propene, butene etc.) However, over the experimental timeframe of the current experiments, absorption at 10.532 microns is dominated by ethylene absorption. High-temperature absorption cross-sections of ethylene and related alkenes (as well as CO_2 and H_2O) and experimental details are discussed in Ren et al. (2012).

Concentration was calculated using Beer's law:

$$I/I_0 = \exp(-k_v P_{total} X_i L) \qquad \text{(Eqn. 1)},$$

where I and I_0 are the transmitted and incident beam intensities, k_v is the absorption coefficient at of the target species at the laser wavelength, P_{total} is the total test gas mixture pressure, X_i is the target species mole fraction, and L is the pathlength. Typical estimated mole fraction uncertainties are ~5%.

Measurements were also performed with the laser tuned off the main absorption line, and with the laser turned off, to verify that there was no significant interfering absorption or emission.

3.3.2 Results and Discussion

3.3.2.1 Shock Tube Measurements of Branched Alkane Ignition Delay Times

Ignition delay times for three branched alkanes: 2,4-dimethylpentane, 2,5-dimethylhexane and iso-octane, were measured behind reflected shock waves. The ignition delay time measurements cover the temperature range of 1313-1554 K, with pressures near 1.5 and 3 atm, equivalence ratios of 0.5 and 1 in 4% oxygen/argon. See Fig. 13. Regression analyses of the data for 2,4-dimethylpentane, 2,5-dimethylhexane, and iso-octane yield the following correlations for ignition delay time as a function of temperature (K), pressure (atm), and equivalence ratio:

2,4-DMP: $\tau_{ign}[s] = 8.4\times10^{-11}P^{-0.61}\Phi^{1.03}\exp(46.6[kcal/mol]/RT)$

2,5-DMH: $\tau_{ign}[s] = 2.1\times10^{-10}P^{-0.60}\Phi^{0.99}\exp(43.4[kcal/mol]/RT)$

Iso-octane: $\tau_{ign}[s] = 1.1\times10^{-10}P^{-0.47}\Phi^{0.86}\exp(45.7[kcal/mol]/RT)$

Comparing the current ignition delay time data of branched alkanes with published values for their normal alkane isomers, it was confirmed that increasing the degree of carbon chain branching lowers the reactivity of the fuel and increases the ignition delay time. See Fig. 14. In

addition, longer ignition delay times were observed for 2,4-dimethylpentane than 2,5-dimethylhexane, confirming the influence on reactivity by changing the straight carbon chain by one carbon for symmetric branched hydrocarbon fuels. The low reactivity and long ignition delay times for branched alkanes were attributed to the high concentrations of propene and iso-butene formed when branched alkanes decompose, as propene and iso-butene reduce the radical pool by consuming OH, O and H and form less reactive species like allyl radical and allene. The ignition delay times of the fuels studied were also seen to increase monotonically with octane number under the current test conditions. Further details of this study can be found in Li et al. (2014).

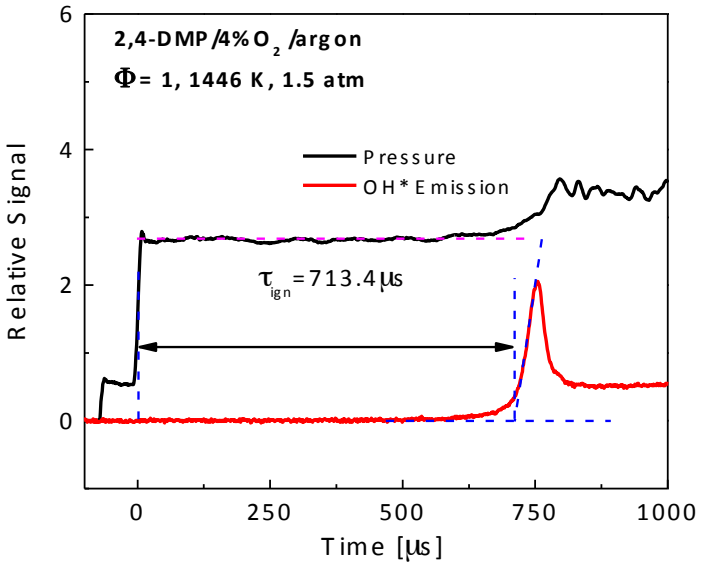

Figure 13. Sample OH* emission and pressure traces during 2,4-dimethylpentane ignition.

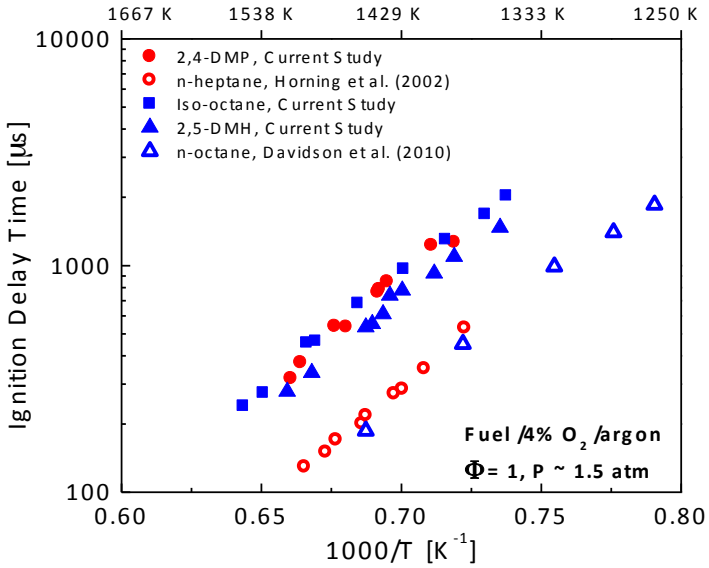

Figure 14. Ignition delay time of different fuels in 4% O_2 /argon with equivalence ratio of 1 and pressure near 1.5 atm.

3.3.2.2 Pyrolysis and Oxidation of Decalin at Elevated Pressures: A Shock-Tube Study

Ignition delay times and ethylene concentration time-histories were measured behind reflected shock waves during decalin oxidation and pyrolysis. Ignition delay measurements were conducted for gas-phase decalin/air mixtures over temperatures of 769 – 1202 K, pressures of 11.7 – 51.2 atm, and equivalence ratios of 0.5, 1.0, and 2.0. See Fig. 15. Negative-temperature-coefficient (NTC) behavior of decalin autoignition was observed, for the first time, at temperatures below 920 K. Current ignition delay data are in good agreement with past shock tube data in terms of pressure dependence but not equivalence ratio dependence. Ethylene mole fraction and fuel absorbance time-histories were acquired using laser absorption at 10.6 and 3.39 μm during decalin pyrolysis for mixtures of 2200 – 3586 ppm decalin/argon at pressures of 18.2 – 20.2 atm and temperatures of 1197 – 1511 K. See Fig. 16. Detailed comparisons of these ignition delay and species time-history data with predictions based on currently available decalin reaction mechanisms are presented, and preliminary suggestions for the adjustment of some key rate parameters are made. Further details on this study can be found in Zhu et al. (2014).

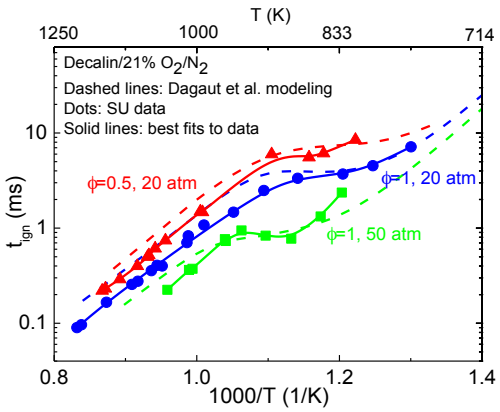

Figure 15. Comparison of measured and originally predicted ignition delay data of decalin/air mixture over 1200 – 770 K at three conditions: ϕ = 0.5, 20 atm; ϕ = 1.0, 20 atm; ϕ = 1.0, 50 atm. Simulations were calculated using the Dagaut et al. 2013 reaction mechanism and constant U, V assumption. NTC behavior is evident at around 940 – 800 K.

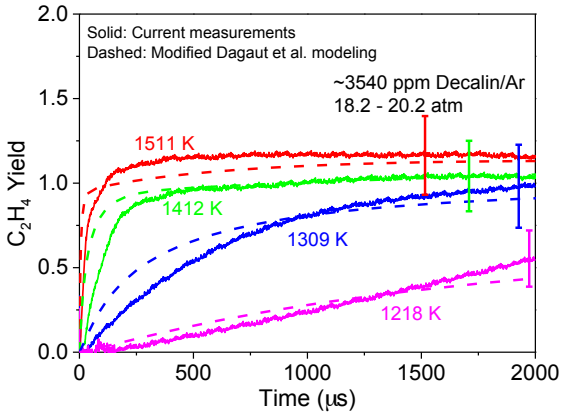

Figure 16. Comparison of measured and newly predicted ethylene yield time-histories during pyrolysis of ~3540 ppm decalin/Ar at 1218 – 1511 K and 18.2 – 20.2 atm. Simulations using the modified Dagaut et al. (2013) modeling described in Zhu et al. 2014.

3.3.2.3 An Experimental and Modeling Study of Propene Oxidation: Ignition Delay Times.

To further understand the ignition characteristics of propene, a series of ignition delay time experiments were performed in a collaborative effort of several universities with six different shock tubes and two rapid compression machines under conditions not previously studied. The present study is the first of its kind to directly compare different shock tubes over a wide range of conditions and greatly expands the data available for validation of propene oxidation models at higher pressures and lower temperatures. Ignition delay times were compared to the predictions of the chemical kinetic mechanism and show relative agreement between mechanism predictions and measurements. See Fig. 17. Further details on this study can be found in Burke et al. (2014).

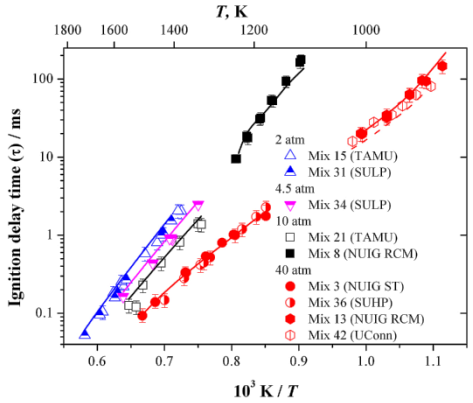

(a), ϕ = 1.0, p = 2, 4.5, 10, and 40 atm C_3H_6/4% O_2.

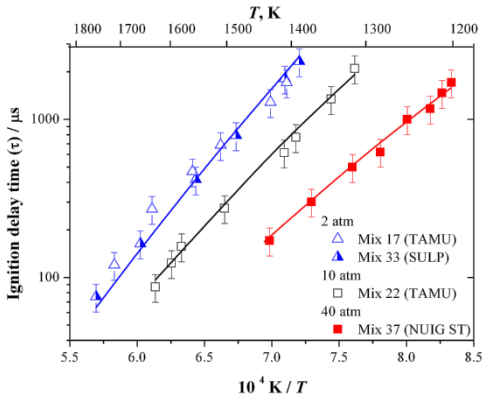

(b)ϕ = 2.0, p = 2, 10 and 40 atm C_3H_6/4% O_2.

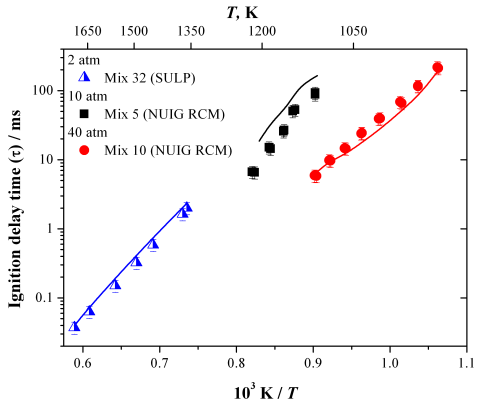

(c) φ = 0.5, p = 2, 10, and 40 atm C_3H_6/4% O_2..

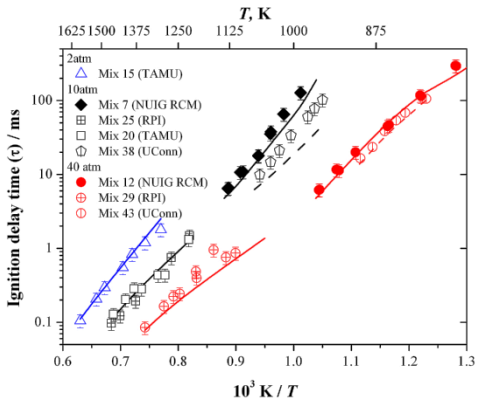

(d)φ = 1.0, p = 2, 10 and 40 atm C_3H_6/12% O_2,.

Figure 17. A comparison of ignition delay times for propene for various equivalence ratios and pressures. SULP: Stanford University Low Pressure Shock Tube; SUHP: Stanford University High Pressure Shock Tube; NUIG RCM: National University of Ireland/Galway Rapid Compression Machine; RPI; Rensselaer Polytechnic Institute Shock Tube; TAMU: Texas A&M University Shock Tube; UConn: University of Connecticut Rapid Compression Machine.

3.3.2.4 Shock Tube and Modeling Study of 2,7-Dimethyloctane Pyrolysis and Oxidation

Ignition delay time measurements in 2,7-dimethyloctane/air were carried out behind reflected shock waves using conventional and constrained reaction volume (CRV) methods. The ignition delay time measurements covered the temperature range 666-1216 K, pressure range 12-27 atm, and equivalence ratio of 0.5 and 1. The ignition delay time temperatures span the low-, intermediate- and high-temperature regimes for 2,7-dimethyloctane (2,7-DMO) oxidation. Clear evidence of negative temperature coefficient behavior was observed near 800 K. See Fig. 18. Fuel time-history measurements were also carried out in pyrolysis experiments in mixtures of 2000 ppm 2,7-DMO/argon at pressures near 16 and 35 atm, and in the temperature range of 1126-1455 K. Based on the fuel removal rates, the overall 2,7-DMO decomposition rate constant can be represented with k = 4.47×105 exp(-23.4[kcal/mol]/RT) [1/s]. Ethylene time-history measurements in pyrolysis experiments at 16 atm are also provided. See Fig. 19. The current shock tube dataset was simulated using a novel chemical kinetic model for 2,7-DMO. The reaction mechanism includes comprehensive low- and high-temperature reaction classes with rate constants assigned using established rules. Comparisons between the simulated and experimental data show simulations reproduce the qualitative trends across the entire range of conditions tested. Further details on this study can be found in Li et al. (in press).

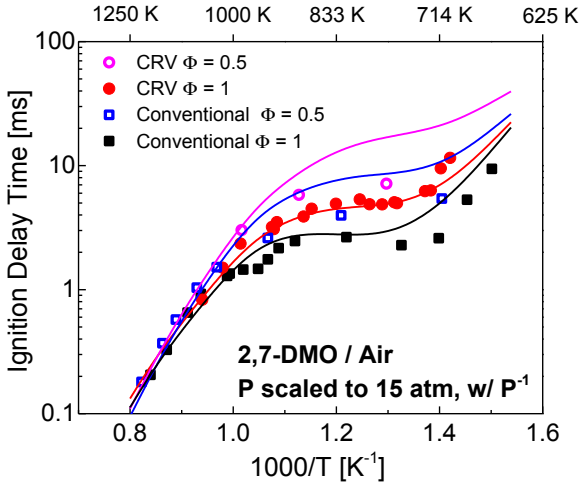

Figure 18. Ignition delay times for 2,7-DMO/ air mixtures at 15 atm and equivalence ratios of 0.5 and 1. Symbols are experiments using CRV and conventional filling strategy. Lines are chemical kinetic simulations using constant-enthalpy/constant-pressure for CRV and constant-volume for conventional filling.

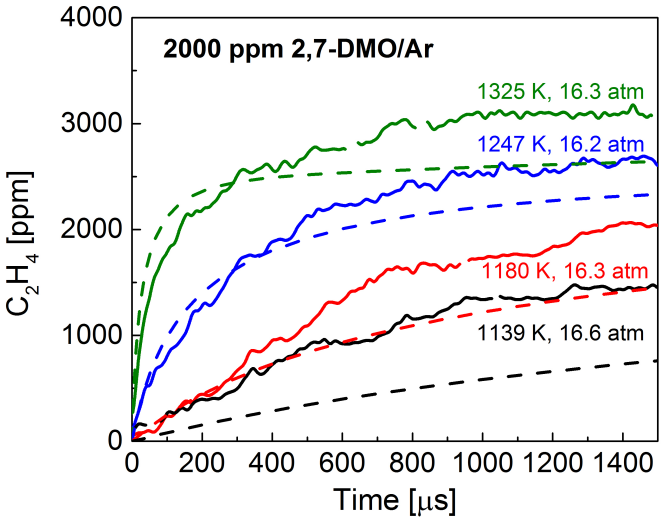

Figure 19. Measured C_2H_4 time-histories (solid lines) at different temperatures, in 2000 ppm 2,7-DMO/Ar mixtures, and constant-pressure kinetic modeling simulations (dashed lines).

3.4 Flame Studies, Princeton University

- Elevated pressure laminar flame speed measurements and analysis (Wu et al. 2012).
    - Cyclohexane/Air: 1, 2, 5, 10, 20 atm, 353 K.
    - Methylcyclohexane/Air: 1, 2, 5, 10, 20 atm, 353 K.
    - Ethylcyclohexane/Air: 1, 2, 5 atm, 353 K.
- Pressure scaling of laminar flame thickness and thermal structure (Zhao et al. 2013).
    - C_5-C_8 *n*-alkanes, 1 - 50 atm, 353 K.
- Turbulent flame speed measurements and scaling (Wu et al. 2014).
    - C_4-C_8 *n*-alkanes, 1 - 5 atm, 353 K, equivalence ratio: $\phi = 0.8, 1.0, 1.4$
    - Turbulence intensity: $u_{rms} = 1$ - 6 m/s, turbulent Reynolds number up to 8,000
- Nonpremixed counterflow ignition in NTC temperature regime (Law and Zhao 2012).
    - *n*-hexane, 1 - 10 atm, strain rate 100 - 1000 1/s.
    - Study on the coupling between NTC chemistry and transport.

3.4.1 Experimental Approach

Conceptually, the design of the apparatus is similar to the previous design for high-pressure flame propagation at room temperature (Tse et al., 2000), modified to allow experimentation with liquid fuels (Kelley et al., 2011) and turbulent flames (Chaudhuri et al. 2012). The apparatus is a double-chambered vessel with one cylindrical chamber radially surrounding the other. The walls of the inner chamber are fitted with a series of holes that can be mechanically opened and closed to allow the union and separation of the gases in the inner and outer

chambers. The outer chamber is covered with silicon electrical heaters, hence enabling it to act as an oven to uniformly heat the inner chamber to around 100^{o}C.

Operationally, after vacuuming both chambers, the connecting holes are closed to seal the inner chamber from the outer chamber. The inner chamber is filled with fuel vapor produced by heating a fuel reservoir, followed by a certified mixture of oxidizer and inert gas, which is also preheated. The outer chamber is filled with a mixture of inert gases to match the density of the gas in the inner chamber. As a secondary check of the equivalence ratio of the mixture, samples of the gas in the tubing connected to the inner chamber are analyzed using a gas chromatograph with a flame ionization detector. All gas samples have been verified to have less than a 2% random error in the equivalence ratio, as is expected based on the gas filling procedure.

After mixing and settling of the gas, the holes between the inner and outer chambers are opened to allow communication between them, while the test gas in the inner chamber is simultaneously spark ignited. This results in a spherical flame that propagates throughout the inner chamber in essentially an isobaric environment before it is quenched upon contacting the inert gases in the outer chamber. For turbulent flame studies, four fans are located at its walls and are driven by motors situated in the outer chamber. Turbulence is generated by these orthogonally positioned fans which continuously run during the entire flame propagation event.

The experimental facility comprises of two measurement systems: (i) High-speed Schlieren system and (ii) High-speed Mie-scattering/PIV system. The Schlieren system uses a high-speed camera with an Hg-vapor lamp as the light source. Using a set of lens and pin-hole, the light from the lamp is converted into a parallel cylindrical beam which enters the chamber through one of the optical windows on the flat side and exits from the other side, and is then focused onto a camera using another set of lens and pin-hole. Due to the sharp density gradient across the flame the light changes it path and creates a sharp intensity gradient on the image. We have recently acquired a Phantom V12.1 high-speed camera, which can operate at rates as high as 1,000,000 fps. It allows us to accurately measure the flame radius as a function of time, $R(t)$. In addition, it also allows detailed visualization of the flamefront morphology therefore identifying the existence of flamefront instability, which is important for accurate determination of laminar flame speeds.

3.4.2 Results and Discussion

(1) Using the above mentioned heated dual-chamber vessel, the propagation speeds of laminar expanding spherical flames of cyclohexane, methylcyclohexane and ethylcyclohexane in mixtures of oxygen/inert were measured, with the corresponding laminar flame speeds extracted from them through nonlinear extrapolation. Measurements were conducted at atmospheric and elevated pressures up to 20 atm. Computational simulations were conducted using the JetSurF 2.0 mechanism, yielding satisfactory agreement with the present measurements at all pressures, with a slight over-prediction at 1 atm. Measurements reveal the following trend of the flame speeds: cyclohexane > *n*-hexane > methylcyclohexane ≈ ethylcyclohexane at all pressures, with the maximum difference being approximately 5% at 1 atm and 13% at 10 atm. Examination of the computed flame structure shows that owing to its symmetric ring structure, decomposition of cyclohexane produces more chain-branching 1,3-butadiene and less chain-terminating propene. On the contrary, a more balanced distribution of intermediates is present in the flames of methylcyclohexane and ethylcyclohexane due to substitution of the alkyl group for H. Details of this study can be found in Wu et al. (2012).

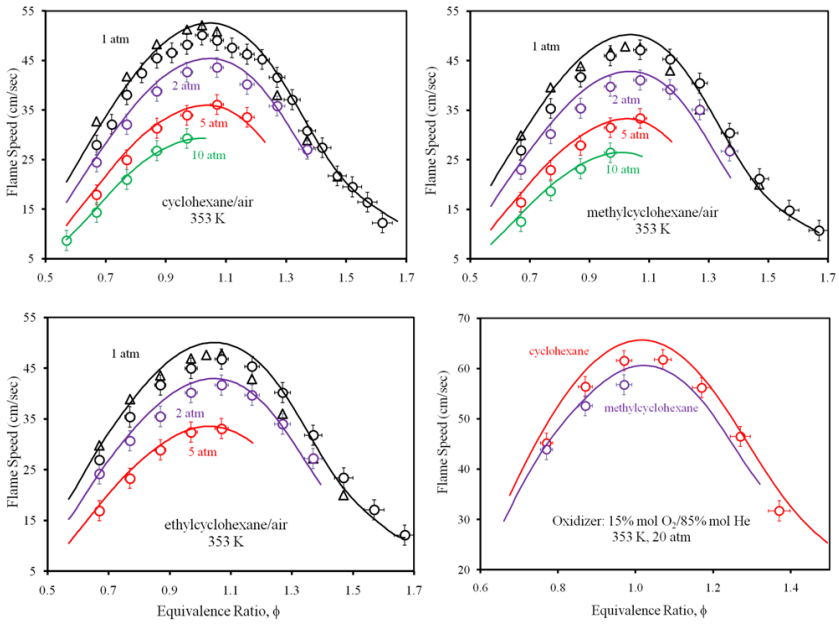

Figure 20. Laminar flame speed measurements for cyclohexane, methylcyclohexane at various pressures from 1 to 20 atm and initial temperature 353K (Wu et al. 2012). Lines are the model predictions by Jet Surf 2.0 (Wang et al. 2010).

(2) Our previous experiments have demonstrated fuel similarity for C_5 to C_8 *n*-alkanes, *i.e.*, the laminar flame speeds and Markstein lengths of these fuels are very close to each other at various pressures. The possible explanation is that large hydrocarbon fuels always rapidly decompose into smaller fuel fragments, whose subsequent oxidation and transport would control the bulk of the flame structure and propagation rate. Such an understanding would significantly simplify/generalize the description of the combustion of large hydrocarbon fuels with similar molecular structures. We investigated fuel similarity along the following two directions.

First, we computationally investigated the fuel similarity for C_5 to C_8 *n*-alkanes systematically in various flame configurations, namely the 1D planar premixed flames, 1D stretched premixed flames, 1D diffusion flames, and 1D unsteady stretched premixed flames. The thermal and chemical structures of these flames, effects of pressure and stretch as well as the large fuel cracking time scale were studied to quantify the criterion for fuel similarity. We found that for laminar premixed flames, the thermal and chemical structures are insensitive to pressure if the flame thickness and burning flux are properly scaled, and fuel similarity always holds for C_5-C_8 *n*-alkanes for all pressures up to 50 atm. For the case of ignition and extinction in nonpremixed systems such as the counterflow and the stagnation flow, for which the ignition/extinction responses seem to be fuel dependent, computation shows that the cause is due to the difference in the diffusive transport such that kinetic similarity is retrieved when the diffusive influence is removed.

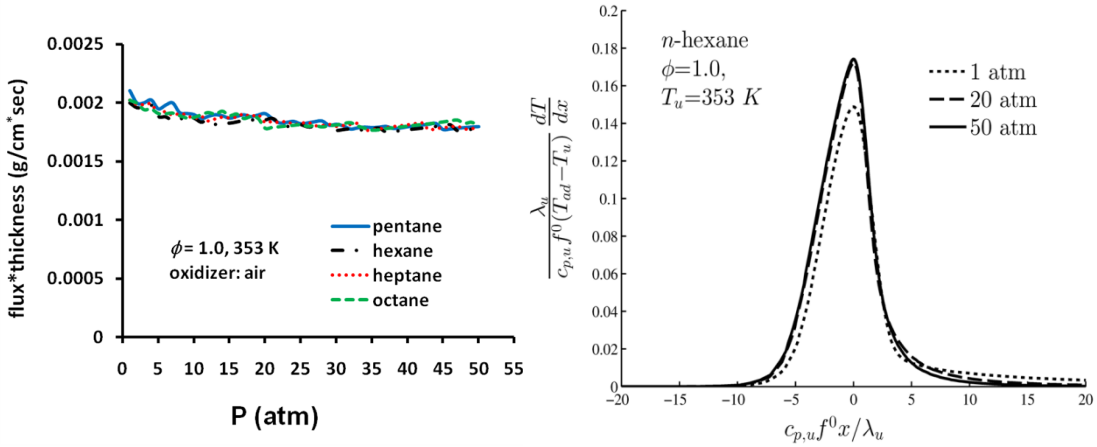

Figure 21. Insensitive pressure dependence of the product of burning flux and laminar flame thickness, and the thermal structure of planar laminar flames for C_5 to C_8 *n*-alkanes at 1, 20 and 50 atm. The calculation used the Jet Surf 2.0 mechanism (Wang et al. 2010).

Second, we experimentally investigated the propagation and the associated propagation speeds of expanding C_4-C_8 *n*-alkane flames in near-isotropic turbulence, from 1 to 5 atm, using the constant-pressure, dual-chamber, fan-stirred vessel. The motivation of the work is to explore whether the previously observed fuel similarity for C_4-C_8 *n*-alkanes for laminar flames also holds for turbulent flames, and to investigate the possible influence of mixture nonequidiffusion on the stretch-affected flame structure especially the occurrence of local extinction. Extensive results show that within the present parametric range of investigation, relevant for the flamelet and thin-reaction zones in the conventional turbulent combustion regime diagram, the turbulent flame speeds of stoichiometric and rich mixtures of these fuels, whose Lewis numbers (*Le*) are close to or smaller than unity, indeed assume similar values at various pressures, equivalence ratios and turbulence intensities. However, the corresponding lean flames, whose *Le* is greater than unity, exhibit strong propensity of local extinction, ostensibly caused by local stretch through the *Le* > 1 mixture nonequidiffusion.

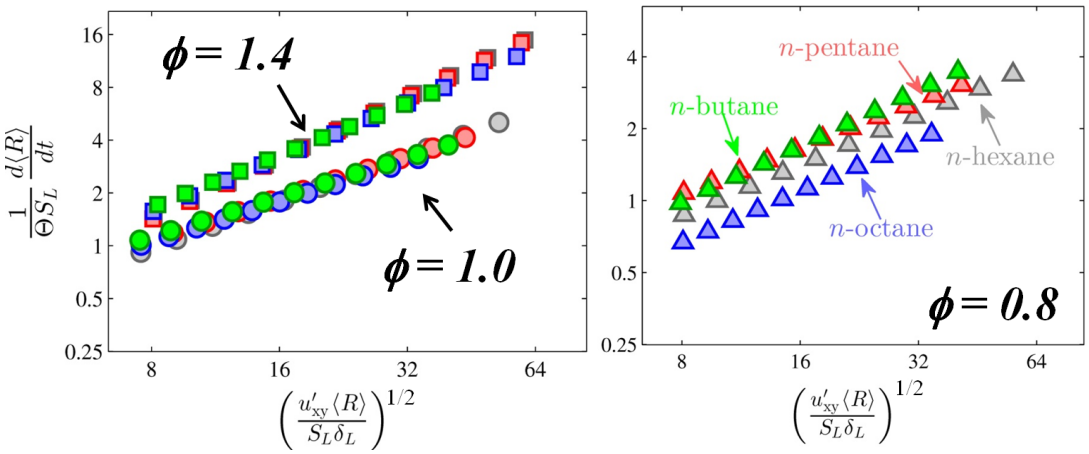

Figure 22. Averaged normalized turbulent flame speeds for *n*-butane, *n*-pentane, *n*-hexane and *n*-octane against a Reynolds number defined based on turbulence intensity, averaged flame radius, laminar flame speed and flame thickness for lean, stoichiometric and rich conditions from 1 to 5 atm.

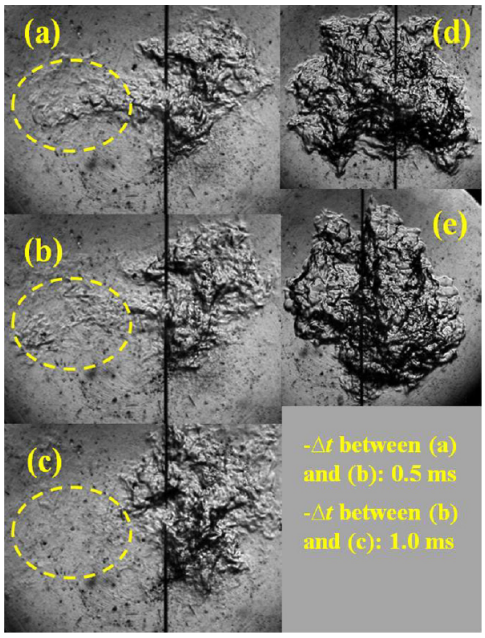

Figure 23. Schlieren images of *n*-octane/air flames at 1 atm with u_{rms} = 5.24 m/s for (a-c) ϕ = 0.8, (d) ϕ = 1.0, (e) ϕ = 1.4 showing the large area of local extinction for ϕ = 0.8, while other conditions do not show such events.

(3) Using *n*-heptane as the model fuel, the role of the Negative Temperature Coefficient (NTC) chemistry on ignition is computationally studied for both homogeneous mixtures and nonpremixed counterflow. For homogeneous mixtures, results show that ignition occurs in two-stages within the NTC temperature regime, with the duration and temperature increment decreasing with increasing initial temperature for the first ignition stage, leading to increased duration of the second ignition stage and thereby the observed NTC-behavior. For the nonpremixed counterflow, results show that a secondary S-curve is developed on the lower branch of the conventional, primary S-curve for sufficiently low strain rates and/or sufficiently high pressures, with its own distinct ignition-extinction turning points. Sensitivity analysis and Chemical Explosive Mode Analysis (CEMA) show that this secondary S-curve is controlled by the low-temperature NTC-chemistry, with heat release negligible for states on its lower branch and discernible for states on its upper branch and hence assuming the characteristics of a weakly-burning flame. The possible existence of one- and two-staged ignition in the counterflow is observed and its dependence on the flow strain rate and system pressure is identified. Further details of this study can be found in Law and Zhao (2012).

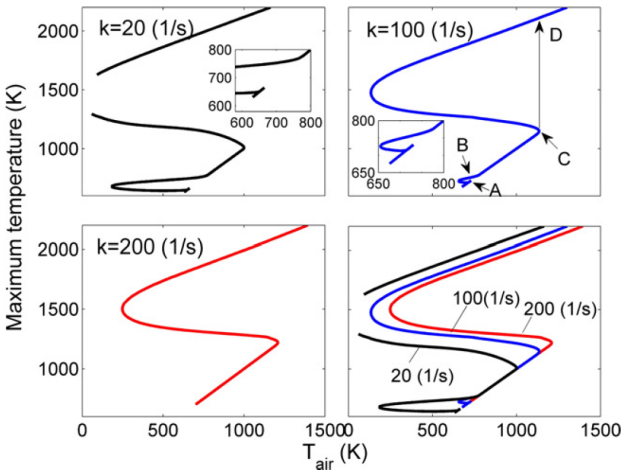

Figure 24. The global response S-curve plotted as maximum temperature versus air side boundary temperature for diffusion counterflow flames at various strain rates. (Law and Zhao, 2012).

3.5 Flame Studies, University of Southern California

- Propagation and extinction of benzene and alkylated benzene flames (Ji et al., 2012)
- Propagation and extinction of cyclopentadiene flames (Ji et al., 2013)
- Development of a piloted premixed jet burner facility for the experimental investigation of high Re number flames of gaseous and heavy liquid fuels.
- Effects of heavy hydrocarbon decomposition on fundamental flame properties.

3.5.1 Propagation and Extinction of Benzene and Alkylated Benzene Flames

Laminar flame speeds and extinction strain rates of benzene, *n*-propylbenzene, toluene, xylenes (*o*-, *m*-, and *p*-), and trimethylbenzenes (1,2,4- and 1,3,5-) flames were determined experimentally in the counterflow configuration under atmospheric pressure and at the unburned temperature of 353 K for the unreacted fuel-containing stream. The experimental results revealed that compared to its alkylated derivatives, benzene/air flames propagate the fastest. The flame chemistry of aromatics was shown to be sensitive to small species chemistry and to the oxidation chemistry of the first few intermediates following the fuel consumption, which are aromatic in nature and fuel-structure dependent. More specifically, it was observed that increased methylation in the fuel results in reduced laminar flame speeds and extinction strain rates caused by the increased radical-radical chain termination through benzyl or benzyl-like radicals. Subtle kinetic differences in the flame chemistry of xylene isomers were noted as well. The different H-shift energy barriers in the methylbenzyl radical appear to provide a logical explanation for the observed differences of the overall reactivity in *o*-, *m*-, and *p*-xylene flames. Such differences, while they have a small but finite effect on laminar flame speeds, they become rather notable for near-extinction non-premixed flames.

Four recent kinetic models were tested against the present experimental data. Comparisons of the experimental and modeling results shows that there exist significant discrepancies among these models and potentially notable uncertainties in the oxidation and pyrolysis kinetics of one-

ring aromatics. Combined with the fact that both the laminar flame speeds and extinction strain rates are greatly sensitive to fuel-specific chemistry, further fundamental kinetic and modeling studies are needed to resolve the observed discrepancies and to establish more accurate reaction kinetics for benzene and its alkylated derivatives.

3.5.2 Propagation and Extinction of Cyclopentadiene Flames

Laminar flame speeds and extinction strain rates of cyclopentadiene/air flames were determined experimentally over an extended range of equivalence ratios in the counterflow configuration under atmospheric pressure and at an elevated unburned mixture temperature. The experimental data are the first ones to be reported and were modeled using available kinetic models. Overall satisfactory agreements were found. Sensitivity analyses revealed that the oxidation of cyclopentadiene/air mixtures depends notably on the chemistry of fuel itself and subsequent intermediates such as cyclopentadienone and cyclopentadienoxy radicals. The analysis revealed further that reactions of small hydrocarbon intermediates resulting from the consumption of cyclopentadienyl have a significant effect on both flame propagation and extinction. Comparing the simulation results, it was concluded that among others, there are uncertainties associated with the consumption pathways of cyclopentadienyl, including $C_5H_5 \Leftrightarrow C_3H_3 + C_2H_2$ and $C_5H_5 + OH \Leftrightarrow C_4H_6 + CO$ that can have a rather significant effect on the prediction of various combustion properties both in homogeneous reactors and flames.

3.5.3 Development of a Piloted Premixed Jet Burner Facility

The burner is shown and schematically described in Fig. 25. It consists of 900 mm long smooth stainless steel tube with and internal diameter, $D = 5.84$ mm and external diameter of 6.35 mm. A fuel lean premixed mixture is flow at high velocity through this tube resulting in fully developed turbulence for the exiting jet. The central tube is surrounded by a co-axial pilot nozzle of larger diameter, $D_{pilot} = 22.9$ mm, and filled with 6.35 mm stainless steel balls. The nozzle is 70 mm long and has an external conical shape though its interior is cylindrical and only

a 0.5 mm step is present 11 mm from the exit. The step holds a 5 mm thick brass perforated plate. The plate has a 22.9 mm outer diameter and 6.35 mm inner diameter with 52 x 1.52 mm holes and is used to stabilize a stoichiometric methane-air flame 7 mm upstream of the central jet. The high temperature products of this pilot flame anchor the jet flame at the nozzle outlet in the shear layer generated among the two flows and allows to ignite the central jet at high *Re* and using lean mixtures.

A large diameter 12.7 mm thick brass perforated plate is co-axially coupled to the base of the pilot nozzle. The plate has an outer diameter of 203 mm and an inner diameter of 24.1 mm with approximately 1800 x 1.52 mm holes that allows the stabilization of flames to thermally shroud the piloted jet from the surrounding environment. At this stage of the study the shroud burner was used only to provide a 0.6 m/s coflow of air around the jet and pilot.

The air flow-rates are regulated using sonic nozzles with accuracy of ±1.0% for the jet and the pilot nozzles and of ±10% for the shroud burner. The fuel flow-rates are controlled with high accuracy using either sonic nozzles or mass flow controllers (Hasting Inc.), for gaseous fuels, or a high accuracy syringe pump (Nexus 6000, Chemyx Inc.) for liquid fuels.

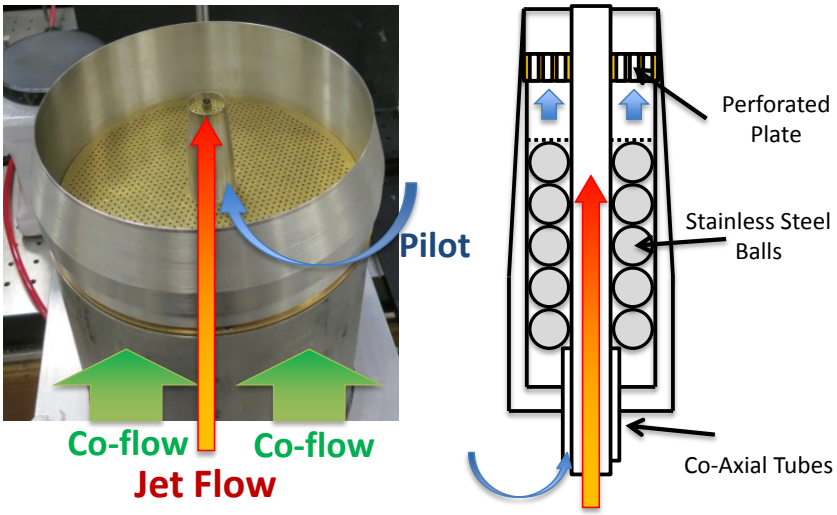

Figure 25. Schematic and picture of piloted premixed jet burner assembly.

A fuel vaporizer system capable of handling flowrates of up to 150 SLPM to attain the desired jet velocities, V_{jet} was used to fully vaporize the liquid fuels, without fuel pyrolysis. Development and verification details of the fuel vaporizer system are mentioned in a separate study in which multiple liquid fuels and gaseous fuels were tested and obtained results consistent with the reactivity of the fuels.

The vaporizer system consists of an inline heater (Omega Engineering Inc.) mounted upstream of two thermostated stainless steel chambers (internal volume 1 liter), connected by a short check section. A commercial nebulizer (Meinhard Inc.) delivers the liquid fuel droplets into the chambers crossed by a constant temperature (423 K) airflow. In addition, an adjustable flow by-pass at the chamber exit regulates the flow traveling through a homemade bubbling bed particle riser to tune the seeding particle density for the particle image velocimetry (PIV) measurements. To reach approximately ambient air temperature at the exit, the heated mixture then flows through a water-cooled counterflowing coaxial heat exchanger before traveling to the burner. The temperature at the burner exit, T_{u}, does not exceed 315 K or dip below ambient for the conditions investigated. The vaporizer and heat exchanger system is used for both gaseous and liquid fuels to maintain consistency in the results.

The experiments were performed for jet Reynolds numbers, $Re_{\text{jet}} = \frac{V_{\text{jet}}D}{\nu}$ up to 60,000. Six fuels with different chemical classification, *n*-heptane (*n*-alkane), 1-hexene (alkene), *iso*-octane (*iso*-alkane), ethyl-cyclohexane (cycloalkane), and toluene (aromatic), as well as methane as a reference were used. Preliminary results obtained using a high-speed camera and an intensifier, suggest that the jet flame structure depends on both the flame diffusivity and reactivity. More specifically, it was shown that the flames are more susceptible to local extinction as the fuel molecular weight increases and as the fuel reactivity decreases. Representative instantaneous flame structures are shown in Fig. 26.

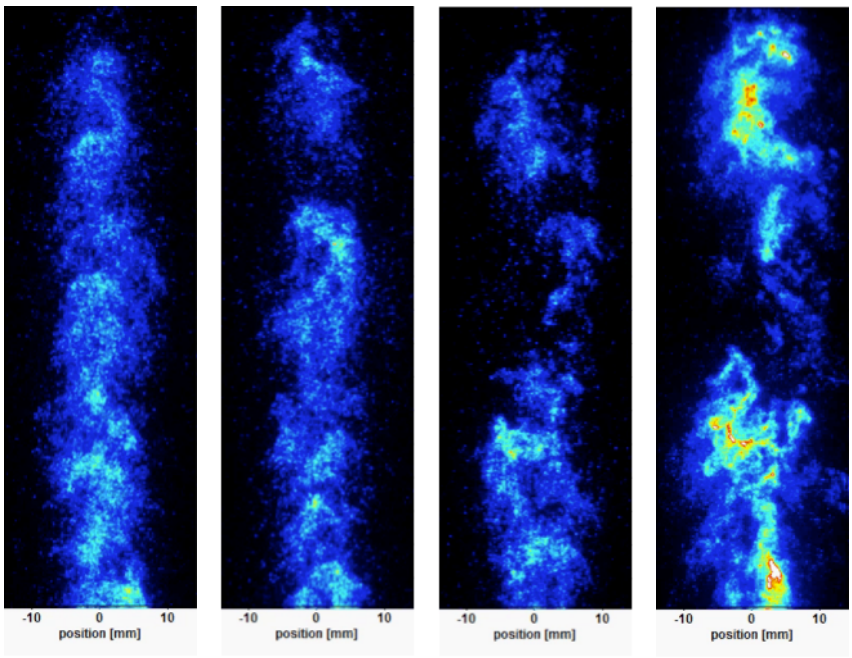

(a) (b) (c) (d)

Figure 26. Instantaneous overlapping CH* + CO_2* chemiluminescence images resolved at 25 KHz for (a) CH_4/air, (b) C_2H_4/air, (c) *n*-C_7H_{16}/air, and (d) toluene/air flames.

3.5.4 Effects of Heavy Hydrocarbon Decomposition on Fundamental Flame Properties

Under intense turbulent conditions encountered in high-speed air breathing propulsion applications, large molecular weight fuels are expected to undergo considerable decomposition in both the free-stream as well as within a thickened preheat zone. Under such conditions, the energy transported from the flame into the unreacted mixture can be partitioned to various extents between chemical and sensible.

Adiabatic, isobaric, partial reaction of *n*-dodecane/air mixtures was modeled under atmospheric pressure at several initial temperatures and equivalence ratios. It was found that fuel decomposition precedes the oxidation of decomposed intermediates. The decomposition occurs over times scales of approximately 1 μs to 10 ms, which are similar to timescales encountered in high Reynolds number turbulent flows. Results indicate that the *n*-dodecane decomposes mainly to form C_2-C_4 alkenes, hydrogen, methane, and some larger alkenes. The mass burning rates and density-weighted extinction strain rates of laminar premixed flames of

the partially reacted mixtures were computed and compared to those of unreacted *n*-dodecane/air mixtures. In all cases, the total enthalpies of the unburned mixtures were identical to each other so as to provide a meaningful comparison.

The results show that under the conditions tested, the impact of partial reaction and fuel decomposition on the mass-burning rate is small and the flame propagation rate is relatively insensitive to the details of fuel decomposition. The density-weighted extinction strain rate was found to be more sensitive to fuel decomposition under lean and stoichiometric conditions. Sensitivity analysis showed that the increased resistance to extinction with the extent of partial reaction of the fuel/air mixture is not caused by reaction kinetics but rather by transport processes as the lighter and more diffusive species such as ethylene facilitate the burning process more efficiently than the parent fuel in stretched flamed. The results are summarized in Fig. 27, in which the effects on fuel decomposition on the mass burning rate and the density-weighted strain rate are shown.

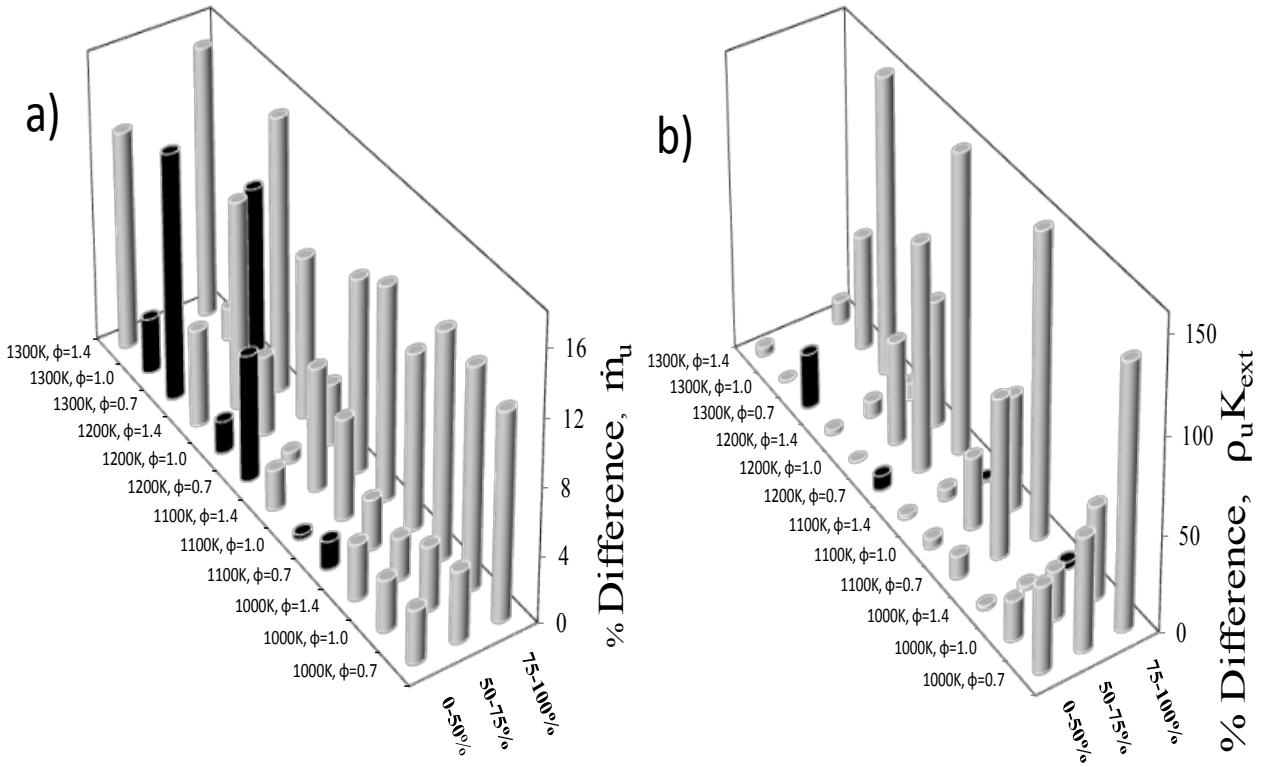

Figure 27. Percent differences in a) mass burning rate and b) density-weighted extinction strain rate from the baseline values, for various equivalence ratios, temperatures and extents of *n*-$C_{12}H_{26}$ decomposition (0-50%: t_{max_nC12}; 50-75%: t_{min_temp}; and 75-100%: t_{zero_C6}). Black cylinders represent negative values and the grey cylinders represent positive values.

3.6 Theoretical and Modeling Studies, University of Southern California/Stanford University

- Kinetic modeling of benzene and alkylated benzene flames (Ji et al., 2012)
- Theoretical study of quantum tunneling in hydrogen transfer isomerization in n-alkyl radical (Sirjean et al. 2012).
- Theoretical studies of the isomerization kinetics of benzylic and methylphenyl type radicals in single-ring aromatics by ab initio electronic structure calculations and reaction theory modeling (Dame and Wang 2013).
- Optimization of a detailed *n*-dodecane model against multispecies time histories of n-dodecane oxidation in shock tube (Banerjee et al. 2014a).
- Development a lumped model for *n*-dodecane pyrolysis and oxidation to test the hybrid-modeling approach (Banerjee et al. 2014b).
- Development of the concept of physics-based approach to real-fuel combustion kinetics leading to the current effort in hybrid model development.

3.6.1 Modeling Approach

3.6.1.1 Physics-Based Hybrid Approach to Modeling Jet Fuel Combustion

Our efforts in the JetSurF development as well as optimization and lumping of *n*-dodecane allow us to gain the following insight:

1. For a majority of the surrogate components the number of unknown or uncertain rate parameters (and pathways) is so large that the problem will remain underdefined for at least a long time;

2. For the above reason further development of detailed models using the fuel surrogate approach will remain an experimental science given the theoretical capabilities currently available to us;

3. Yet, the dimensionality of the mixture condition space remains too large to be explored experimentally even for a five-component surrogate because of potential kinetic coupling among the surrogate components during the pyrolysis and oxidation processes;

4. The wide variation of the initial decomposition products during the pyrolysis of jet fuels and their surrogate components suggests that only a careful tuning of a surrogate composition based on actual measured jet fuel decomposition products will recover the correct kinetic behavior during jet fuel pyrolysis. Hence, a surrogate-based approach where only physical-chemical parameters of jet fuel are matched is unlikely to accurately duplicate the chemical behavior of the fuel.

5. Given the size of the detailed reaction models (O(10^3) species and O(10^4) reactions), it is a daunting task, if not impossible, to reduce the model to a approximately 35 species.

The above considerations motivated us to seek alternative approaches to the solution of the underlying problem.

3.6.1.2 Tunneling in Hydrogen-Transfer Isomerization of *n*-Alkyl Radicals

The role of quantum tunneling in hydrogen shift in linear heptyl radicals is explored using multi-dimensional, small-curvature tunneling method for the transmission coefficients and a potential energy surface computed at the CBS-QB3 level of theory. The purpose was to understand the generalized behavior governing the isomerization of alkyl radicals generated during the initial stage of fuel pyrolysis. Several one-dimensional approximations, including the Wigner, Skodje and Truhlar, and Eckart methods, were compared to the multi-dimensional results. The Eckart method was found to be sufficiently accurate in comparison to the small-curvature tunneling results for a wide range of temperature, but this agreement is in fact fortuitous and caused by error cancellations. High-pressure limit rate constants were calculated

using the transition state theory with treatment of hindered rotations, and Eckart transmission coefficients for all hydrogen transfer isomerizations in *n*-pentyl to *n*-octyl radicals. Rate constants are found in good agreement with experimental kinetic data available for *n*-pentyl and *n*-hexyl radicals. In the case of *n*-heptyl and *n*-octyl, our calculated rates agree well with limited experimentally derived data. Several conclusions made in the experimental studies of Tsang et al. (2009) are confirmed theoretically: older low-temperature experimental data, characterized by small pre-exponential factors and activation energies, can be reconciled with high-temperature data by taking into account tunneling; at low temperatures, transmission coefficients are substantially larger for H-atom transfers through a five-membered ring transition state than those with six-membered rings; channels with transition ring structures involving greater than 8 atoms can be neglected because of entropic effects that inhibits such transition. The set of computational kinetic rates were used to derive a general rate rule that explicitly accounts for tunneling. The rate rule is shown to reproduce closely the theoretical rate constants. The work is reported in Sirjean et al. (2012).

3.6.1.3 Isomerization Kinetics of Benzylic and Methylphenyl Type Radicals in Single-Ring Aromatics

Mutual isomerization through H-atom shifts in benzylic and methylphenyl type radicals are examined for toluene, and *o*-, *m*-, and *p*-xylene isomers. Our particular aim is to explain the differences of the reactivity observed for xylene isomers in flames. In the high temperature pyrolysis and oxidation of toluene, three possible methylphenyl radical isomers can be formed (2-, 3-, and 4-methylphenyl). The 2-methylphenyl radical may undergo a facile isomerization to benzyl through a four-membered ring critical structure—a pathway not accessible to 3- and 4-methylphenyl. Electronic structure calculations show that 2-methylphenyl isomerization to benzyl is preferred energetically by at least 20 kcal/mol over other possibilities. Monte Carlo RRKM/Master Equation simulations illustrate that, at temperatures $\geq$ 1200 K, and for almost all pressures, the 2-methylphenyl radical has a lifetime of only several microseconds, whereas 3- and 4-methylphenyl radicals have a substantially longer lifetime, allowing them to react with other species, including molecular oxygen, during toluene oxidation. This is also found to be the

case for all dimethylphenyl radicals in the three xylene isomers. As a result, the structure of the xylene isomers and specifically the number of H atoms immediately adjacent to the methyl groups can have a direct impact on their high-temperature oxidation and appear to explain the observed differences in xylene oxidation behind reflected shock waves and in laminar premixed flames. This work is reported in Dames and Wang (2013).

3.6.1.4 Optimization of *n*-Dodecane Model and Development and Test of a Lumped Model Approach

The development of large chemical kinetic models for single liquid hydrocarbon fuels often benefits from the principle of chemical similarity to estimate reaction rate parameters. For example, the JetSurF 1.0 model (Sirjean et al. 2009) for the pyrolysis and oxidation of *n*-alkanes up to *n*-dodecane is assigned with a set of class rules. Within each class, the rate parameters are assumed to be equal and their values based on known rates available, typically for smaller hydrocarbon species. This approach satisfactorily reproduced all experimental observations of *n*-heptane combustion and the laminar flame speed of n-dodecane, but it does not provide accurate predictions of shock tube data available for *n*-dodecane. Notably, there exist notable differences between simulated multi-species time histories and those observed behind reflected shock waves [Davison et al. 2011]. In this work, we employ the method of uncertainty quantification and minimization using polynomial chaos expansion (MUM-PCE) [Sheen & Wang, 2011] to explore the origin of the experimental and model discrepancy. The results suggest that, in certain cases, the chemical similarity principle is inadequate for rate parameter estimation and requires rate optimization against experimental observations specifically made for a given fuel. Optimization was carried on JetSurF1.0, using targets that included *n*-$C_{12}H_{26}$, OH, C_2H_4, CO_2 and H_2O time histories measurement obtained from shock heating of a near-stoichiometric *n*-dodecane-oxygen-argon mixture (Series 1) [Davison et al. 2011]. Additionally, a set of atmospheric pressure *n*-dodecane/air laminar flame speed data (Series 2) [You et al. 2009), and two sets of ignition delay times for *n*-dodecane/air mixtures (Series 3) [Vasu et al. 2009] are included in the analyses. The results indicate that (1) the available experimental data may be reconciled by the JetSurF1.0 model; (2) the optimization yielded a reaction model notably more predictive against the

experimental data considered than the unoptimized model; (3) the rate rule is adequate only in generating initial guesses for the reaction model of the *n*-alkane series, but it requires systematic optimization and uncertainty minimization in order to better reproduce the experimental data. To further test the validity of the optimization approach and procedure, the optimized model was tested against species time profiles of *n*-dodecane pyrolysis and oxidation measured in flow reactor (see, section ??.? – Bowman's part) with satisfactory results. A part of this work has been reported in Tangko et al. (2011). The full report will be given in Banerjee et al. (2014a).

3.6.1.5 A Lumped Approach to Modeling *n*-Dodecane Oxidation at High Temperatures

In this work, a procedure was developed that can carry out lumping of the reactions of the pyrolysis of large hydrocarbon fuels into a just few reaction steps. The lumping procedure uses the following assumptions: (1) the reaction starts by C-C fission in the fuel molecule (*n*-dodecane as the example) leading to the formation of a range of alkyl radicals; (2) the reactant hydrocarbon depletes by H-abstraction reactions with key radical species in a reactive system; (3) the alkyl radicals are in chemical equilibrium; and (4) the equilibrated alkyl radicals undergo beta scission to produce a range of critical pyrolysis products, including CH_3, C_2H_5, C_2H_4, C_3H_6, and 1-C_4H_8. The reactions of these C_1-C_4 small species may be described by a detailed reaction model that is generally well established. Test results show that the lumping approach reproduces the behaviors as predicted by the detailed model over a wide range of conditions, including the flow reactor measurements for *n*-dodecane pyrolysis and oxidation. The approach taken and the test done here paved an important path to describing the combustion chemistry of real, multicomponent jet fuels using a physics-based approach. The full report will be given in Banerjee et al. (2014b).

3.6.1.6 Development of Alternative Approaches to Jet Fuel Kinetics

The JetSurF effort suggests that the pyrolysis of large hydrocarbon fuels leading to smaller molecular fragments precedes the oxidation of the resulting fragments. The two reaction processes are separable in time scales. In flames, the pyrolysis and oxidation zone are expected to separate spatially. The disappearance of the fuel is accompanied by the production of several small intermediates that are transported into the flame zone to undergo oxidation. For thermodynamic and chemical kinetic reasons, the pyrolysis of a jet fuel in the flame front or during the induction time of an ignition process yields only a handful of species that may include H_2, CH_4, C_2H_4, C_3H_6, 1-C_4H_8 (1-butene), *i*-C_4H_8 (isobutene), benzene and toluene. Past studies also suggest that during high-temperature fuel oxidation the rate-limiting steps are largely the oxidation of pyrolysis products. The above considerations led us to take a hybrid approach to chemistry modeling of jet fuel combustion, namely, a physics-based to jet fuel pyrolysis leading to the production of a handful of molecular fragments, followed by a detailed description of the reaction kinetics for the oxidation of pyrolysis fragments by detailed reaction model. The kinetic rates and composition of the pyrolysis products can be determined experimentally.

4.0 References

Banerjee, S., Tangko, R., Sheen, D. A., Wang, H., Bowman, C. T. "*n*-Dodecane Pyrolysis and Oxidation in a Flow Reactor: Experiment, Model Optimization and Test," *manuscript in preparation,* (2014a).

Banerjee, S., Wang, H., Bowman, C. T. "A Hybrid Modeling Approach to High-Temperature Oxidation of n-Dodecane," *manuscript in preparation,* (2014b).

Bray, K. N. C, Cant R. S. 1991 "Some applications of Kolmogorov turbulence research in the field of combustion," *Proc R Soc London A* **434**, 217–227.

Burke, S. M., Burke, U., McDonagh, R., et al., "An Experimental and Modeling Study of Propene Oxidation," *Combustion and Flame*, in press (DOI: 10.1016/j.combustflame.2014.07.032).

Chaudhuri S., Wu F., Zhu D. L., Law C. K., "Flame speed and self-similar propagation of expanding turbulent premixed flames", *Physical Review Letters*, **108**, pp. 044503 (2012).

Corrubia, J.A., Farid, F., Cernansky, N.P., Miller, D.L., "The Low to Intermediate Temperature Oxidation of n-Propylcyclohexane in a Pressurized Flow Reactor," Paper No. 2A12 presented at the *7th U.S. National Combustion Meeting*, Atlanta, GA, March 20-23, (2011).

Dagaut, P., Ristori, A., Frassoldati, A., Faravelli, T., Dayma, G., Ranzi, E., *Proceedings of the Combustion Institute* **34**, pp. 289-296 (2013).

Dames, E., Wang, H. "Isomerization kinetics of benzylic and methylphenyl type radicals in single-ring aromatics," *Proceedings of the Combustion Institute*, **34**, pp. 307-314 (2013).

Damköhler, G. 1940 "Der Einfluss der Turbulenz auf die Flammengeschwindigkeit in Gasgemischen," *Z. Elektrochem. und Angewandte Physikalische Chemie* **46**, 601-626.

Davidson, D. F., Ranganath, S. C., Lam, K.-Y., Liaw, M., Hong, Z., Hanson, R. K., *Journal of Propulsion and Power* **26**, pp 280-287 (2010).

Davidson, D.F., Hong, Z., Pilla, G.L., Farooq, A., Cook, R.D., Hanson, R.K., "Multi-Species Time-History Measurements during *n*-Dodecane Oxidation behind Reflected Shock Waves," *Proceedings of the Combustion Institute* **33**, pp. 151-157 (2011).

Farid, F., Corrubia, J.A., Cernansky, N.P., Miller, D.L., "Oxidation of 2,7-Dimethyloctane and *n*-Propylcyclohexane in the Low to Intermediate Temperature Regime with a Pressurized Flow Reactor," Paper No. 1A15 presented at the 8*th U.S. National Combustion Meeting*, Park City, UT, May 19-22, (2013).

Horning, D., Davidson, D. F., Hanson, R. K., *Journal of Propulsion and Power* **18**, pp. 363-371 (2002).

Ji, C.-S., Dames, E., Wang, H., Egolfopoulos, F. N. "Propagation and extinction of benzene and alkylated benzene flames," *Combustion and Flame* 1**59**, pp. 1070-1081 (2012).

Ji, C.-S., Zhao, R., Li, B., Egolfopoulos, F. N. "Propagation and extinction of cyclopentadiene flames," *Proceedings of the Combustion Institute* **34**, pp. 787-794 (2013).

Kelley, A.P., Smallbone, A.J., Zhu, D.L., Law, C.K., "Laminar Flame Speeds of C_5 to C_8 *n*-Alkanes at Elevated Pressures: Experimental Determination, Fuel Similarity, and Stretch Sensitivity," *Proceedings of the Combustion Institute* **33**, pp. 963-970 (2011).

Klingbeil, A. E., Jeffries, J. B., Hanson, R. K., *Measurement Science and Technology* **17**, pp. 1950-1957 (2006).

Koert, D.N., Cernansky, N.P., "A Flow Reactor for the Study of Homogeneous Gas-Phase Oxidation of Hydrocarbons at Pressures up to 20 atm (2 MPa), *Measurement Science and Technology* 3 pp. 607-613, (1992).

Kurman, M.S., "The Preignition Oxidation Chemistry of n-Decane and n-Dodecane in a Pressurized Flow Reactor and Their Use as Jet Fuel Surrogate Components," Ph.D. Dissertation, Drexel University, Philadelphia, PA, (2010).

Law, C. K., Zhao P., "NTC-affected ignition in nonpremixed counterflow," *Combustion and Flame* **159**, pp. 1044-1054 (2012).

Li, S., Sarathy, S. M., Davidson, D. F., Hanson, R. K., Westbrook, C. K., "Shock Tube and Modeling Study of 2,7-Dimethyloctane Pyrolysis and Oxidation," *Combustion and Flame*, in press.

Ren, W., Davidson, D. F., Hanson, R. K., *International Journal of Chemical Kinetics* **44**, pp. 423-432 (2012).

Sheen, D.A., Wang, H., "Kinetic Uncertainty Quantification and Minimization Using Polynomial Chaos Expansions," *Combustion and Flame*, **158**, pp. 2358-2374 (2011).

Sirjean, B., Dames, A., Sheen, D.A., You, X.-Q., Sung, C., Holley, A.T., Egolfopoulos, F.N., Wang, H., Vasu, S.S., Davidson, D.F., Hanson, R.K., Pitsch, H., Bowman, C.T., Kelley, A., Law, C.K., Tsang, W., Cernansky, N.P., Miller, D.L., Violi, A., Lindstedt, R.P., "JetSurF version 1.0 – A high-temperature chemical kinetic model of *n*-alkane oxidation with quantifiable uncertainties," http://melchior.usc.edu/JetSurF/Version1_0 /Index.html. September 15, 2009.

Sirjean, B., Dames, E., Wang H., Tsang, W. "Tunneling in hydrogen transfer isomerization of *n*-alkyl radical," *Journal of Physical Chemistry A* **116**, pp. 319-332 (2012).

Tangko, R., Sheen, D.A., Wang, H., "Combustion Kinetic Modeling Using Multispecies Time-Histories in Shock-Tube Oxidation of *n*-Dodecane," 7th US National Meeting of Combustion, Atlanta, Georgia, paper 2A18, March 20-23, 2011.

Tsang, W., McGivern, W.S., Manion, J.A. "Multichannel decomposition and isomerization of octyl radicals," *Proceedings of the Combustion Institute* 32 (2009) 131-138.

Tse S. D., Zhu D. L., Law C. K., "Morphology and burning rates of expanding spherical flames in H_2/O_2/inert mixtures up to 60 atmospheres", *Proceedings of the Combustion Institute* **28**, pp. 1793-1800 (2000).

Vasu, S.S., Davidson, D.F., Hong, Z., Vasudevan, V., Hanson, R.K., "*n*-Dodecane Oxidation at High Pressures: Measurements of Ignition Delay Times and OH Concentration Time Histories," *Proceedings of the Combustion Institute* **32** pp. 173-180 (2009).

Wang, H., Dames, E., Sirjean, B., Sheen, D.A., Tangko, R., Violi, A., Lai, J.Y.W., Egolfopoulos, F.N., Davidson, D.F., Hanson, R.K., Bowman, C.T., Law, C.K., Tsang, W., Cernansky, N.P., Miller, D.L., Lindstedt, R.P., "JetSurF version 2.0 – A high-temperature chemical kinetic model of *n*-alkane (up to *n*-dodecane), cyclohexane, and methyl-, ethyl-, *n*-propyl and *n*-butyl-cyclohexane oxidation at high temperatures," http://melchior.usc.edu/JetSurF/JetSurF2.0. September 19, 2010.

Wu F., Kelley A. P., Law C. K., "Laminar flame speeds of cyclohexane and mono-alkylated cyclohexanes at elevated pressures," *Combustion and Flame* 159, pp. 1417-1425 (2012).

Wu F., Saha A., Chaudhuri S., Law C. K., "Propagation speeds of expanding turbulent flames of C_4 to C_8 *n*-alkanes at elevated pressures: experimental determination, fuel similarity, and stretch-affected local extinction," *Proceedings of the Combustion Institute* 35, in press (2014).

You, X.Q., Egolfopoulos, F.N., Wang H., "Detailed and Simplified Kinetic Models for *n*-Dodecane Oxidation: The Role of Fuel Cracking in Aliphatic Hydrocarbon Combustion," *Proceedings of the Combustion Institute* **32**: 403-410 (2009).

Zhao P., Liang W., Wu F., Law C. K., "Fuel similarity of laminar flames of C_5-C_8 n-alkanes", Technical Meeting of the Eastern States Section of the Combustion Institute, Clemson University, South Carolina, October 13-16 (2013).

Zhu, Y., Davidson, D. F., Hanson, R. K., "Pyrolysis and Oxidation of Decalin at Elevated Pressures: A Shock Tube Study," *Combustion and Flame* **161**, pp. 371-383 (2014).

5.0 Personnel

This research was performed by the PIs, a number of research associates, and a number of graduate research assistants.

6.0 Archival Publications

Banerjee, S., Tangko, R., Sheen, D. A., Wang, H., Bowman, C. T. "*n*-Dodecane Pyrolysis and Oxidation in a Flow Reactor: Experiment, Model Optimization and Test," *manuscript in preparation,* (2014a).

Banerjee, S., Wang, H., Bowman, C. T. "A Hybrid Modeling Approach to High-Temperature Oxidation of n-Dodecane," *manuscript in preparation,* (2014b).

Burke, S. M., Burke, U., McDonagh, R., et al., "An Experimental and Modeling Study of Propene Oxidation," *Combustion and Flame*, in press.
DOI: 10.1016/j.combustflame.2014.07.032.

Corrubia, J.A., "The Low to Intermediate Temperature Oxidation of n-Propylcyclohexane at Elevated Pressure in a Pressurized Flow Reactor", M.S. Thesis, Drexel University, Philadelphia PA, (2014).

Corrubia, J.A., "Low to Intermediate Temperature Oxidation and Pyrolysis of JP-8 Surrogate Components", Ph.D. Dissertation, Drexel University, Philadelphia PA, in preparation, (2015).

Corrubia, J.A., Farid, F., Cernansky, N.P., Miller, D.L., "Pyrolysis of *n*-decane and *n*-dodecane in a Pressurized Flow Reactor," in preparation (2014).

Corrubia, J.A., Farid, F., Cernansky, N.P., Miller, D.L., "The Low to Intermediate Temperature Oxidation of *n*-Propylcyclohexane in a Pressurized Flow Reactor," in preparation (2014).

Dames, E., Wang, H. "Isomerization kinetics of benzylic and methylphenyl type radicals in single-ring aromatics," *Proceedings of the Combustion Institute*, **34**, pp. 307-314 (2013).

Farid, F., "Low Temperature Oxidation Chemistry of iso-Cetane in a Pressurized Flow Reactor“, M.S. Thesis, Drexel University, Philadelphia PA, (2014).

Farid, F., Ph.D. Dissertation, " Oxidation and Pyrolysis of Straight-Chain and Branched Paraffins in the Low and Intermediate Temperature Regimes ", Drexel University, Philadelphia PA, in preparation, (2015).

Farid, F., Corrubia, J.A., Cernansky, N.P., Miller, D.L., “The Low to Intermediate Temperature Oxidation of *iso*-Cetane/*n*-Decane Mixtures in a Pressurized Flow Reactor,” in preparation (2014).

Ji, C.-S., Dames, E., Wang, H., Egolfopoulos, F. N. “Propagation and extinction of benzene and alkylated benzene flames,” *Combustion and Flame* 1**59**, pp. 1070-1081 (2012).

Ji, C.-S., Zhao, R., Li, B., Egolfopoulos, F. N. “Propagation and extinction of cyclopentadiene flames,” *Proceedings of the Combustion Institute* **34**, pp. 787-794 (2013).

Law C. K., Zhao P., “NTC-affected ignition in nonpremixed counterflow,” *Combustion and Flame* **159**, pp. 1044-1054 (2012).

Li, S., Campos, A., Davidson, D. F., Hanson, R. K., “Shock Tube Measurements of Branched Alkane Ignition Delay Times,” *Fuel* **118**, pp. 398-405 (2014).

Li, S., Sarathy, S. M., Davidson, D. F., Hanson, R. K., Westbrook, C. K., “Shock Tube and Modeling Study of 2,7-Dimethyloctane Pyrolysis and Oxidation,” *Combustion and Flame*, in press.

Liu W., Law C. K., Lu T. F., “Multiple criticality and staged ignition of methane in the counterflow,” *International Journal of Chemical Kinetics* **41(12)**, pp. 764-776 (2009).

Lu T. F., Yoo C. S., Chen J. H., Law C. K., “Three-dimensional direct numerical simulation of a turbulent lifted hydrogen jet flame in heated coflow: a chemical explosive mode analysis,” *Journal of Fluid Mechanics* **652(1)**, pp. 45-64 (2010).

Ranzi E., Frassoldati A., Grana R., Cuoci A., Faravelli T., Kelley A. P., Law C. K., "Hierarchical and comparative kinetic modeling of laminar flame speeds of hydrocarbons and oxygenated fuels," *Progress in Energy and Combustion Science* 38, pp. 468-501 (2012).

Sirjean, B., Dames, E., Wang H., Tsang, W. "Tunneling in hydrogen transfer isomerization of *n*-alkyl radical," *Journal of Physical Chemistry A* **116**, pp. 319-332 (2012).

Wu F., Kelley A. P., Law C. K., "Laminar flame speeds of cyclohexane and mono-alkylated cyclohexanes at elevated pressures," *Combustion and Flame* 159, pp. 1417-1425 (2012).

Wu F., Saha A., Chaudhuri S., Law C. K., "Propagation speeds of expanding turbulent flames of C_4 to C_8 *n*-alkanes at elevated pressures: experimental determination, fuel similarity, and stretch-affected local extinction," *Proceedings of the Combustion Institute* 35, in press (2014).

Zhu, Y., Davidson, D. F., Hanson, R. K., "Pyrolysis and Oxidation of Decalin at Elevated Pressures: A Shock Tube Study," *Combustion and Flame* **161**, pp. 371-383 (2014).

7.0 Interactions/Transitions

The PIs had several meetings with Dr. Tim Edwards and other personnell of AFRL/WP during the reporting period. In these meetings numerous aspects of the ongoing work regarding practical jet fuels as well as the relevant neat hydrocarbons were discussed. Additionally, the possibility to extend the reach of JetSurF model and apply it for models of soot formation in gas turbine engines was addressed.